Marine Pollution Bulletin
February 2022, Volume 175, Pages 113131 (15p.)
https://doi.org/10.1016/j.marpolbul.2021.113131
https://archimer.ifremer.fr/doc/00737/84932/

Combined effects of ocean warming and acidification on the larval stages of the European abalone *Haliotis tuberculata*

Kavousi Javid [1, *], Roussel Sabine [1], Martin Stephane [2, 3], Gaillard Fanny [3], Badou Aicha [4], Di Poi Carole [5], Huchette Sylvain [6], Dubois Philippe [7], Auzoux-Bordenave Stéphanie [2, 8]

[1] Univ Brest, CNRS, IRD, Ifremer, LEMAR, Plouzane, France
[2] Sorbonne Université, 4 place Jussieu, Paris 75005, France
[3] UMR 7144 “Adaptation et Diversité en Milieu Marin” (AD2M), CNRS/SU, Station Biologique de Roscoff, Roscoff, Cedex, 29680, France
[4] Direction Generale Deleguee a la Recherche, l'Expertise, la Valorisation et l'Enseignement (DGD REVE), Muséum National d'Histoire Naturelle, Station marine de Concarneau, Concarneau 29900, France
[5] Ifremer, LEMAR UMR 6539 UBO/CNRS/IRD/Ifremer, Argenton, France
[6] Ecloserie France Haliotis, Kerazan, Plouguerneau 29880, France
[7] Laboratoire de Biologie Marine, Université Libre de Bruxelles, CP160/15, 1050, Brussels, Belgium
[8] UMR “Biologie des Organismes et Ecosystèmes Aquatiques” (BOREA), MNHN/CNRS/SU/IRD, Muséum National d'Histoire Naturelle, Station Marine de Concarneau, Concarneau 29900, France

* Corresponding author : Javid Kavousi, email address : javid.kavousi@gmail.com

Abstract :

This study examined the physiological responses of the larval stages of Haliotis tuberculata, an economically important abalone, to combined temperature (17 °C and 19 °C) and pH (ambient pH and −0.3 units, i.e., +200% increase in seawater acidity) in a full factorial experiment. Tissue organogenesis, shell formation, and shell length significantly declined due to low pH. High temperature significantly increased the proportion of fully shelled larvae at 24 h post-fertilization (hpf), but increased the proportion of unshelled larvae at 72 hpf. Percentage of swimming larvae at 24 hpf, 72 hpf and 96 hpf significantly declined due to high temperature, but not because of low pH. Larval settlement increased under high temperature, but was not affected by low pH. Despite the fact that no interaction between temperature and pH was observed, the results provide additional evidence on the sensitivity of abalone larvae to both low pH and high temperature. This may have negative consequences for the persistence of abalone populations in natural and aquaculture environments in the near future.

Highlights

► Combined impacts of ocean acidification and warming on the larvae of the European abalone were investigated. ► No interactive impact of temperature and pH was recorded. ► Tissue organogenesis, shell formation, and shell length significantly declined due to low pH. ► High temperature significantly increased the proportion of fully shelled larvae at 24 hpf, but increased the proportion of unshelled larvae at 72 hpf. ► High temperature increased the settlement rate of the larvae.

Keywords : Ocean acidification, Global warming, Climate change, Marine mollusks, Abalone larvae

1. Introduction

Increased CO_2 concentrations due to anthropogenic activities have led to increased oceanic CO_2 absorption, resulting in a phenomenon called ocean acidification (OA) that is concurrent with ocean warming (OW). Current projections suggest that by the year 2100, the average sea surface temperature will increase by 1 °C–3 °C and the water pH will drop by 0.1 to 0.3 units (i.e., +30% to +200% increases in acidity; IPCC, 2014). OA has particularly deleterious impacts on marine calcifiers that produce calcium carbonate ($CaCO_3$) skeletons (Kroeker et al., 2013; Parker et al., 2013). These minerals are experiencing unprecedented decreases in their saturation states due to ongoing OA. This has a suppressive, narcotic effect and causes acidosis, which impairs many physiological processes (Feely, 2004; Pörtner, 2008; Doney et al., 2009). In contrast, the impacts of increased temperatures due to OW can stimulate physiological processes until they reach a threshold (Pörtner, 2010; Byrne et al., 2011).

The combined impacts of OA and OW have been addressed with contrasting responses, such that the effects of OA and OW are either exacerbated (e.g., Di Santo, 2015; D'Amario et al., 2020; Zittier et al., 2018; Rodolfo-Metalpa et al., 2011) or ameliorated (e.g., Kroeker et al., 2014; Davis et al., 2013; Knights et al., 2020; García et al., 2015; Jiang et al., 2018) in the presence of the other stressor . Meta-analyses have suggested that the combined impacts of OA and OW on species physiology are especially devastating for the larval stages of many species (Przeslawski et al., 2015; Kroeker et al., 2013), presenting a major bottleneck for population persistence under changing oceanic conditions (Przeslawski et al., 2015). As a result, the responses of these early stages to combined OA and OW are now being paid greater attention (Przeslawski et al., 2015). Temperature and OA-related factors, such as

pH, are among the paramount environmental factors that dictate the survival, morphology, physiology, and behavior of marine larvae, and in particular, calcifying larvae (Przeslawski et al., 2015). Among all of the marine calcifiers studied so far, mollusk larvae are the most vulnerable to the effects of OA (Przeslawski et al., 2015; Kroeker et al., 2013).

The recent marine mollusks include over 43,000 recognized species that includes some of the major $CaCO_3$ producers (Rosenberg, 2014) fulfilling crucial ecosystem functions, such as creating habitat structures and food sources for benthic species (Parker et al., 2013). Therefore, any negative impacts from environmental drivers can result in high ecological and economic consequences (Narita et al., 2012). Abalones are important mollusks that have high ecological and commercial values, and also provide food for human beings (Cook, 2016; Huchette and Clavier, 2004). However, their natural populations have experienced severe declines due to overexploitation (Micheli et al., 2008; Kashiwada and Taniguchi, 2007) and environmental disturbances such as OW and bacterial diseases (Cook, 2016; Travers et al., 2009; Huchette and Clavier, 2004; Morales-Bojórquez et al., 2008). Since abalone aquaculture is expanding worldwide, understanding the effects of global change drivers on abalone physiology is an important issue for the management of abalone populations in natural and aquaculture environments (Morash and Alter, 2015).

Early life-history stages of abalones are negatively affected by OA and show a high percentage of deformed larvae under low-pH conditions (Byrne et al., 2011; Crim et al., 2011; Guo et al., 2015; Kimura et al., 2011; Zippay and Hofmann, 2010; Wessel et al., 2018; Swezey et al., 2020). Other negative responses that have been reported in abalones in response to temperatures higher than their physiological limit during development include abnormal appearance, reduced growth, and trochophore mortality (e.g., Leighton, 1974; Pedroso, 2017). Although several studies have shown larval abalones to be highly sensitive to OA (Santander, 2018; Crim et al., 2011; Tahil and Dy, 2016; Guo et al., 2015; Wessel et al., 2018), the combined effects of OA and OW are still not understood (Gao et al., 2020). Based on the limited data available, OA and OW may have deleterious impacts on abalone populations. Indeed, *Haliotis coccoradiata* embryos were dramatically affected by a combination of high temperatures ($+2$ to $+4$ °C compared with control 20 °C) and acidified conditions (-0.4 to -0.6 pH units), with only a small percentage surviving (Byrne et al., 2011).

Haliotis tuberculata is a commercially important species in Europe, for which rearing over the whole life cycle is controlled in aquaculture (Huchette and Clavier, 2004; Courtois de Viçose et al., 2007). As for most marine mollusks, abalone species display a pelago-benthic life cycle with a larval planktonic stage followed by a critical metamorphosis into the benthic juvenile, making the specie highly sensitive to environmental changes (Byrne et al. 2011). The impacts of OA on all stages of the European abalone, *Haliotis tuberculata* have been recently studied (Wessel et al., 2018; Auzoux-Bordenave et al., 2020; Avignon et al., 2020). All the aforementioned studies reported adverse impacts of OA on *H. tuberculata*, especially on the shell growth and calcification. However, *H. tuberculata* larvae were more impaired by OA than was any other life stage, showing significantly adverse effects in survival rate, morphology and development, growth rate and shell calcification (Wessel et al., 2018). While the impacts of OA on abalone larvae are worrying enough, high temperatures present another emerging threat for *H. tuberculata* populations (Travers et al., 2009; Huchette and Clavier, 2004). Furthermore, there is a lack of knowledge on how climate change will modify *H. tuberculata* larval settlement, behavior and physiology in early life stages.

In this study, we investigated the combined effects of OA and OW on the early life stages of *H. tuberculata* in a full factorial experiment. Abalone larvae were exposed to four OA and OW scenarios: ambient (pH 8.0 and 17 °C); combined (pH 7.7 and 19 °C); and individual effect scenarios (pH 8.0 and 19 °C; pH 7.7 and 17 °C) throughout the five days of larval development. We focused on three key larval stages: the trochophore stage, characterized by the set-up of the larval shell at 24 h post-fertilization (hpf); the mature veliger stage (72 hpf); and the premetamorphic veliger stage (96 hpf), which is the last pelagic life stage before larval settlement (Jardillier et al., 2008; Auzoux-Bordenave et al., 2010). To better understand both the individual and combined effects of OA and OW, we investigated several biological parameters involved in growth, physiology and behavior throughout the larval development cycle of *H. tuberculata*.

2. Materials and methods

2.1. Abalone larvae production

The parental *H. tuberculata* stock was composed of wild broodstock (3 females and 7 males) collected from Saint Quay Portrieux (Brittany, France), and farmed abalones (4 females and 5 males) collected from an offshore sea-cage structure at the France *Haliotis* abalone farm (48°36′50 N, 4°36′3 W; Plouguerneau, Brittany, France). Mixing wild and farmed broodstocks prevent inbreeding and production of enough larvae for the experiment. In France *Haliotis* farm, after a 10-month period in nursery tank, abalone are placed in sea-cages and raised with similar environmental conditions as the wild abalone apart the protection from the predator attacks and high density until the age of 4 years. They are fed with algae collected on the shore, and submitted to the same temperature and pH as the wild broodstock.

The wild and farmed abalones were were given time to acclimatize to the farm's conditions over three months with natural running seawater maintained at 15 °C and pumped twice a day from the sea, with ad libitum feeding to assure optimal reproduction maturity. Spawning was induced following usual procedures. Briefly, abalones were detached from the rearing aquarium and placed individually into 5-L buckets. Spawning was stimulated with ultraviolet light while gradually heating the filtered seawater from 18 °C to 21 °C over the course of 1 h. Abalones were allowed to spawn for a maximum of 5.5 h from the start of the experiment. Once spawned, the eggs were pooled and then divided into 12 batches. Spermatozoa from each of the 12 males (one male per batch of eggs) were added separately to avoid spermatic competition (Harney et al., 2018) at an optimal sperm concentration of approximately 100,000 spermatozoa per egg (Huchette et al., 2004). After 1 h, the fertilized eggs were pooled again and their density was estimated under a binocular microscope. The pooled fertilized eggs were then divided into 12 samples of 900,000 embryos per batch and transferred to the 12 hatching boxes.

2.2. Experimental design

To study the individual and combined impacts of OA and OW, we applied a full factorial design of two temperatures (17 °C [low] and 19 °C [elevated]) and two pH values (8.0 [high] and 7.7 [low]; with three replicate tanks per treatment (12 tanks in total; Fig. 1). We considered 17 °C to be the ambiant ("low") temperature, as it was the temperature experienced by abalones during the summer reproduction period in Northern Brittany. According to Gac et al. (2020), temperature in the Northern Brittany reach maximal summer value of 17 °C and present short-term variability of 0.1 to 0.4 °C mainly related to the tidal cycle and the day-time. Similarly, the high pH corresponded to the naturally occurring pH during autumn in Northern Brittany (Qui-Minet et al., 2018), that is, the high pH in this experiment was the ambient pH of the seawater pumped into the France *Haliotis* site. The high temperature and low pH conditions were chosen based on the global projections for the coming decades (IPCC, 2014). We chose the worst-case pH and temperature scenarios; however, the high temperature treatment in this study is about 1 °C lower than the worst scenarios predicted for 2100. Abalone larvae were exposed to the experimental conditions from 1 h post-fertilization until they reached the premetamorphic veliger stage.

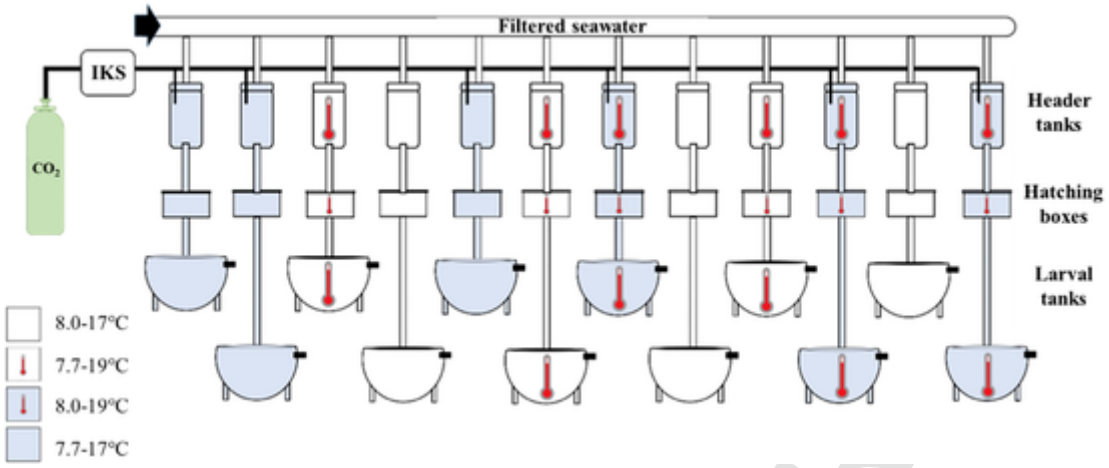

Fig. 1. Simplified design of the experimental system showing the flow of filtered seawater from the header tanks, the styrene hatching boxes, and the 350-L larval tanks (12 in total). Seawater exited the system via the black outflow at the top of larval tanks. IKS is a pH-regulated electrovalve system. The four treatments are indicated using two colors (white and blue to differentiate high and low pH, respectively) and a red thermometer for high temperatures. (For interpretation of the references to colour in this figure legend, the reader is referred to the web version of this article.)

The temperature was controlled using two central heating systems. For the 17 °C treatment and pre-heating of the 19 °C treatment, we used an Aquahort Ltd. Heat Pump (26 kW; THP26-3). To reach 19 °C, we supplemented this pump with a Charot Heat Pump (6 kW; 4911 type). Each replicate was composed of three parts: I) a food-safe plastic head tank (60 L), in which water of the appropriate temperature and CO_2 level was premixed and homogenized with a bubbling system; II) a food-safe 22.5-L hatching box (30 cm × 50 cm × 15 cm), which was supplied with reduced-flow running water from the head tank to avoid flushing the eggs out while maintaining the desired pH and temperature. This box harbored the fertilized eggs to allow them to hatch within the first 18 h. An evacuation pipe was connected to the rearing tank to allow automatic larval transfer once the larvae could swim; this transfer was completed over 4 h. III) A 350-L epoxy-coated larval tank, which was supplied by the head tank, to rear hatched larvae that had left the hatching box. Natural 3-μm filtered seawater was allowed to run through the tanks at all times (open circuit). To prevent larvae from leaving the tanks, a 40-μm net was placed at the outflow. The flow rate from the head tanks to the rearing tanks was between 200 and 400 mL · min^{-1}. All tanks were exposed to an artificial photoperiod of 12 h light:12 h dark, which was provided at a light intensity of 900–1000 lx at the water surface using 68-W natural spectrum light-emitting diode (LED) lamps (Solar Natur, JBL). As pre-settlement abalone larvae are lecithotrophic (non-feeding), they were not fed during the experiment.

2.3. Carbonate chemistry and pH control

Carbonate chemistry and pH control were monitored according to the methods of Avignon et al. (2020). Low-pH seawater was provided by bubbling CO_2 (Air Liquide, Paris, France) into the tanks through electrovalves regulated by a pH-stat system (Aquastar, IKS Computer System, Karlsbad, Germany) (one electrovalve and bubbling CO_2 system per header tank). The desired low-pH value was adjusted to be 0.3 units lower than the high pH, corresponding to natural pH fluctuations along the Northern Brittany coast (the total scale (pH_T) range of 7.9–8.2; Qui-Minet et al., 2018). The values of the pH-stat system were adjusted from daily measurements of the electromotive force in the header tanks using a pH meter (Metrohm 826 pH mobile, Metrohm AG, Herisau, Switzerland) with a glass electrode (Metrohm Ecotrode Plus, Metrohm AG, Herisau, Switzerland). The electromotive force values were converted to pH units on the pH_T after calibration with Tris-HCl and 2-aminopyridine-HCl (AMP) buffers (Dickson et al., 2007).

Temperature and salinity were measured daily using a portable conductivity meter (ProfiLine Cond 3110, WTW, Oberbayern, Germany). Total alkalinity (A_T) was measured twice (n = 12 and n = 9) from 50-mL samples taken from each experimental tank. Seawater samples were filtered through 0.7-μm Whatman GF/F membranes, immediately poisoned with mercury chloride, and stored in a dark place at room temperature for later analysis.

A_T was determined from approximately 50 g of weighed samples using a potentiometric titration at 25 °C with 0.1 M HCl and using a Titrino 847 plus Metrohm. The balance point was determined by the Gran method (Gran, 1952) according to Haraldsson et al. (1997). The accuracy of this method was ±2 μmol · kg^{-1} and was verified by Certified Reference Material 182, provided by A. Dickson (Scripps Institute of Oceanography, University of South California, San Diego, United States). The seawater carbonate chemistry analysis included dissolved carbonate (CO_3^{2-}), bicarbonate (HCO_3^-), dissolved inorganic carbon (DIC), pCO_2, aragonite saturation state (Ω_{ar}), and calcite saturation state (Ω_{calc}); these were determined by entering the values of pH_T, A_T, temperature, and salinity into CO2SYS software (Lewis and Wallace, 1998) using constants from Mehrbach et al. (1973) as refitted by Dickson and Millerro (1987).

2.4. Hatching success

Under pH 8.0 and 17 °C, trochophore larvae typically hatch at 18–20 hpf (Jardillier et al., 2008). To estimate the percentage of larvae that hatched in the 12 experimental hatching boxes, we collected all of the unhatched larvae that were deposited at the bottom of the hatching boxes at 24 hpf, after the hatched larvae could swim and had evacuated to the 350-L rearing tank. Nine 1-mL replicates were sampled from a 5-L bucket and fixed with 90% ethanol. Then, the total number of unhatched larvae per tank was counted under a binocular microscope. To estimate the percent hatching success of each tank, we used Eq. (1).

$$\frac{\text{number of swimming larvae at 24 hpf}}{(\text{number of swimming larvae at 24 hpf} + \text{number of unhatched larvae})} \times$$

2.5. Morphometric assessment and percentage of swimming larvae

The post-embryonic developmental stages of *H. tuberculata* were explained in detail by Jardillier et al. (2008) and Auzoux-Bordenave et al. (2010). Our morphometric measurements were focused at 24 and 72 hpf, which corresponded to the free-swimming trochophore and ma-

ture veliger stages, respectively. Therefore, only the swimming larvae in the tank water column that corresponded to these larval stages were sampled for further analyses.

The development timing of the larvae was investigated under a binocular microscope at 24, 72, and 96 hpf to verify the larval stages before sampling . At 24 and 72 hpf, the total number of larvae swimming in each tank was estimated from six 10-mL replicates per tank (n = 18 per treatment). For morphometric, birefringence, and scanning electron microscopy (SEM) analysis, 10–15 L of seawater containing larvae was collected from each tank and filtered through a 40-μm sieve, then aliquoted into 15-mL tubes. Larvae were concentrated at the bottom of each sample by adding few drops of 70% ethanol; then, the samples were fixed and stored in 70% ethanol for polarized light microscopy and SEM analysis. At 96 hpf, all of the swimming larvae were filtered out of the 350-L tank using a 40-μm sieve and placed into buckets containing 5 L of seawater adjusted to the same temperature and pH as in their respective treatments. The percentage of swimming larvae at 96 hpf was calculated from eight 1-mL samples (n = 24 per treatment). The percentage of swimming larvae was calculated at 24 hpf, 72 hpf and 96 hpf as the total number of swimming larvae in the 350-L tank at each time point divided by the initial number of larvae that hatched.

2.6. Slide preparation for morphometric and birefringence analysis

To study morphometric characteristics and birefringence, 12 slides per larval stage (1 replicate per experimental tank) were prepared with the ethanol-fixed larvae (Wessel et al., 2018). Approximately 100 larvae were whole-mounted in about 500 μL of glycerol. All ethanol was removed before the samples were transferred into the glycerol. The slides were kept at room temperature for 5 to 10 min to allow any remaining ethanol to evaporate and let the larvae settle. Six spots of vacuum gel were deposited at the corners and middle edges of a square coverslip to prevent the larvae from being crushed. After placing the coverslip over the glycerol, the slides were gently sealed with clear nail polish. Each slide contained 150 larvae per treatment per larval stage.

Table 1
Semi-quantitative morphological categories of abalone larvae at 24 and 72 hpf. Categories were based on shell formation and soft tissue morphogenesis according to the developmental cycle of *Haliotis tuberculata* at 17 ± 0.5 °C (Jardillier et al., 2008).

Score	Shell formation	Soft tissue morphogenesis
2	Normal shell	Tissues normally developed
1	Shell partially and/or abnormally developed	Abnormal or partially developed
0	No shell	Undeveloped

The first 50 larvae that were observed per slide, regardless of their orientation, shape, and development, were photographed for morphological analysis with an Olympus binocular microscope (Olympus, Hamburg, Germany) under phase contrast and under polarized light. The same microscope was equipped with polarizing filters for the birefringence analysis. To avoid bias, a coding system was used to prevent the person taking pictures and analyzing the photos from learning which slides corresponded to the particular treatments. All images were taken with a digital camera (DS-Ri1, Nikon) at 20× magnification and a 40-ms exposure. Images were analyzed in ImageJ software (1.52a).

2.7. Morphometric analysis

Larval development, shell formation, and shell size were analyzed for larvae lying on the lateral side (n = 125–133 larvae per treatment). We used semi-quantitative categorizations to analyze larval development, whereby each larva was scored on a scale from 0 to 2 as one of three morphological categories (Table 1; Fig. 2).

The maximum larval length (24 hpf) or total shell length (72 hpf) were measured using ImageJ software and used as indicators of larval size, with all individuals lying on the lateral side (Fig. 3). The mean length of larvae from each tank was calculated, and the average value for all tank replicates was presented as the mean larva size for each treatment (n = 3 tanks per treatment).

2.8. Birefringence analysis

We measured birefringence on a scale of 0–255 under cross-polarized light using an Olympus microscope, according to the method described by Wessel et al. (2018). Cross-polarized light that passes through $CaCO_3$ (an anisotropic material) is double-refracted, and shells with higher $CaCO_3$ content double-refract more light. Therefore, birefringence intensity can be used as a proxy for evaluating shell mineralization (Noisette et al., 2014). Birefringence was measured for at least 120 larvae per treatment at 24 and 72 hpf using ImageJ. The mean grayscale level (in pixels) was determined for each area of the larval shell showing birefringence, i.e., two zones for 24 hpf larvae, and three zones for 72 hpf larvae.

2.9. Scanning electron microscopy

Larvae stored in 70% ethanol were used for SEM analysis (four larvae per treatment). Samples were dehydrated in a series of increasingly concentrated ethanol solutions (90%, 95%, and 100%) and were critical point dried with liquid CO_2. Finally, the samples attached to the SEM stubs were gold-coated and observed at 5 kV with a SIGMA 300

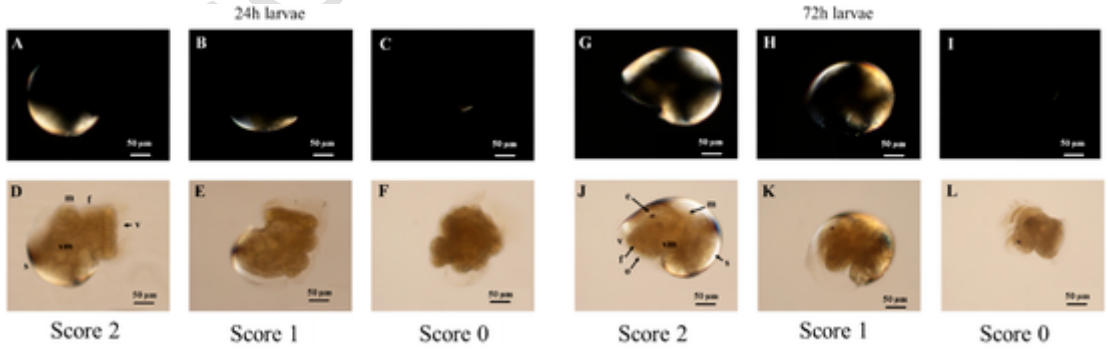

Fig. 2. Polarized microscope (A–C and G–I) and light microscope (D–F and J–L) images showing the morphological variables used for larval scoring at 24 h post-fertilization (hpf; left) and 72 hpf (right). A and G Larvae with normal shell development (score = 2; the shell field covers the posterior area of the larval body, including the light half-circled area). B and H Partially and/or abnormally developed shell (score = 1). C and I Larvae with no shell development (score = 0). D Larvae at 24 hpf with normal tissue development (score = 2). J Larvae at 72 hpf with normal tissue development (score = 2). E and K Partially and/or abnormally developed larvae (score = 1). F and L Underdeveloped larvae (score = 0). velum (v), mantle (m), shell (s), foot (f), visceral mass (vm), eyes (e), and operculum (o).

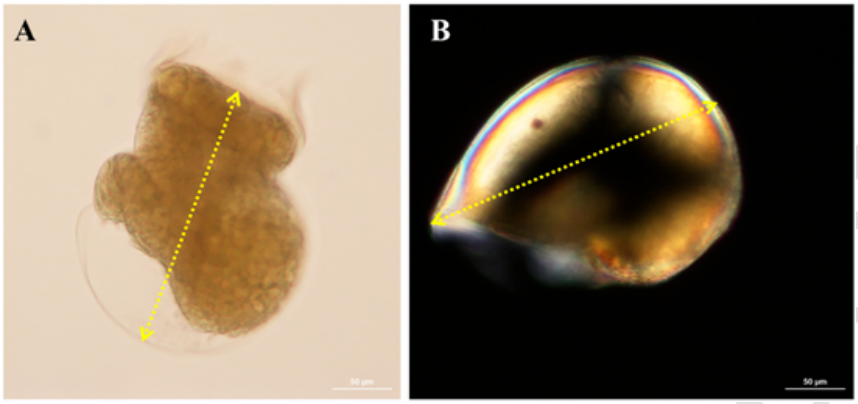

Fig. 3. Larval length measured at A 24 h post-fertilization (hpf) and B 72 hpf. Arrow heads show the two ends of the measured lengths. Scales are 50 μm.

FE-SEM scanning electron microscope (Plateau Technique de Microscopie Electronique, MNHN, Concarneau, France).

2.10. Larval swimming behavior

At 72 hpf, a 1-L sample was taken from each 350-L tank by carefully dipping a plastic bucket into the middle of the tank and filling it to its maximum capacity. The bucket was covered with a lid to minimize CO_2 exchange and ensure pH stability. The samples were kept in insulated boxes to maintain their respective temperature treatments while they were transported (< 45 min) to the Institut Français de Recherche pour l'Exploitation de la Mer (IFREMER) experimental station (Argenton, France). Upon arrival, the buckets were placed in water baths adjusted to their respective treatment temperatures to recover from their transport. After 2 h, the samples were examined for the behavioral analysis.

The pH treatments were randomly selected for behavioral analysis, alternating the elevated and low temperatures. Before filtration, each bucket's temperature and pH were measured to ensure that the treatment conditions had been maintained. Larvae were concentrated in a 40-μm sieve and collected with a pipette. A total of 10–20 larvae per sample were distributed into 24-well plates. The wells (16 mm in diameter) were filled with 500 μL of natural seawater with the same temperature and pH as in their original treatment (n = 3 or 4 replicates per tank). All larvae were allowed to habituate for 5 min prior to starting the test. Videos were recorded in the DanioVision Observation Chamber® (Noldus Information Technology, the Netherlands) using a camera (Basler, GigE) fitted with a 55-mm lens that was positioned 15 cm away from the microplate. Each video was recorded for 30 s at 30 frames per second and 1920 × 1080 resolution. All processed videos were analyzed under completely treatment-blind conditions using the software EthoVision XT 13.0 (Noldus Information Technology, Wageningen, the Netherlands). This software tracked active larval swimming for a maximum of 16 larvae simultaneously (not exceeded in our case) within a selected area. To reduce uncertainty, we pre-set a few criteria that were followed for each video. For example, if the larvae hit the walls of the well or if they collided, the behavioral variables after the collision were excluded from further analysis. Therefore, only larvae that were detected for at least 10 consecutive seconds without interruption were used in our analyses. If a larva did not move for 30 consecutive seconds, then no signal was detected by the program and a value of zero was indicated for the different behavioral variables of that larva.

The distance moved was measured as the distance (mm) that each larva traveled by the center point of the subject over 30 s. The mean velocity ($mm \cdot s^{-1}$) was calculated by dividing the distance moved by the unit of time (s). The mean meander ($deg \cdot mm^{-1}$) was calculated as the mean change in a larva's direction of movement relative to its distance moved; this provided an indication of how convoluted the larva's trajectory was.

2.11. Larval metabolism

At 72 hpf, larval respiration rates were determined using closed incubations in acrylic respirometry chambers (Engineering and Design Plastics Ltd., Cambridge, UK). We carried out six incubations for each experimental tank: three incubations with larvae in 120-mL respirometry chambers, and three incubations with larvae-excluded seawater (control) in 80-mL respirometry chambers. We applied a correction to compensate for the differences in chamber volume. About 100 L of live larvae were siphoned from the experimental tanks and resuspended in 1 L of filtered seawater from the experimental tanks to reach a density of 100 larvae mL^{-1}. The incubation chambers that contained larvae were filled with this same larval resuspension, whereas the control chambers were filled with filtered seawater from the experimental tanks. The chamber temperatures were maintained at the larval culture temperature during the incubations, either at room temperature (17 °C) or at an high temperature (19 °C) using a circulating water bath. The respiration rates were calculated from the measured differences in oxygen concentration during each incubation using a noninvasive fiber-optical system (FIBOX 3, PreSens, Regensburg, Germany) made up of an optical fiber and a reactive oxygen spot attached to the inner wall of each chamber. The reactive oxygen spots were calibrated using a 0% oxygen buffer that was prepared by dissolving 10 g of Na_2SO_3 into 1 L of seawater, and a 100% oxygen buffer that was prepared by bubbling air into 1 L of seawater for 20 min to achieve oxygen saturation. Oxygen consumption was measured over 1.5 to 2 h and checked for linearity. Respiration rates were corrected for oxygen consumption in the controls and normalized to the number of larvae ($\mu mol\ O_2 \cdot larva^{-1} \cdot h^{-1}$).

After each incubation (n = 9 per treatment), the exact number of larvae per chamber was determined from six 100-μL sample replicates per chamber that were distributed into a six-well plate.

For two of the three replicate incubations per experimental tank (n = 6 per treatment), the larvae were removed from the chambers, rinsed with distilled water to remove salt, and filtered through a pre-weighed Whatman GF/F 0.7-μm membrane. Filters containing larvae were dried in an oven at 60 °C for 48 h to determine their DW. The relative CaCO3 content (%) was calculated from the ash weight after burning at 550 °C for 5 h and the DW of each sample ($g\ CaCO3 \cdot g^{-1}$ DW larvae).

2.12. Larval settlement

Larval settlement, which involves attachment to the substrate to achieve metamorphosis, occurs about 4 days after fertilization in *H. tuberculata* at 17 ± 0.5 °C (Jardillier et al., 2008). Therefore, the larval

settlement rate (%) was evaluated using premetamorphic 96 hpf veliger larvae. Twenty-four glass aquaria (20 cm W × 35 cm L × 20 cm H) were filled with 12 L of seawater at the same temperature and pH as in the original tanks. Temperatures were maintained by using a water bath set at 19 °C for half of the aquaria. The other 12 aquaria were left at the low temperature of 17 °C. We used a closed system with no water renewal to prevent the larvae from escaping from the small aquaria. Therefore, the pH of the acidified treatment could not be adjusted during the 24-h settlement period. As a result, the pH_T increased from 7.69 ± 0.04 at the beginning of the test to 7.86 ± 0.03 at the end of the test. In each aquarium, we installed two 10 cm × 15 cm vertical polycarbonate plates, one covered with the green microalga *Ulvella lens*, and one without *U. lens*. *U. lens* is one of the major inductive cues for the settlement of abalone larvae (De Viçose et al., 2010, 2012; Daume et al., 2004), and the absence of such cues can substantially reduce larval settlement rates (Searcy-Bernal et al., 1992; Slattery, 1992; Daume et al., 1999). After estimating the density of the larvae, a 1-mL volume was distributed using a pipette into two aquarium pseudo-replicates (n = 6 per treatment). The volume was adjusted to create a similar density of the larvae in each aquarium. After about 24 h, we used a binocular microscope to record the number of larvae that had settled on each plate. The water in each tank was filtered using a 40-μm filter to collect any larvae that were unsettled or that had attached to the sides and bottom of the tank. We applied low-pressure seawater to remove any larvae that had attached to the tank. The larvae that were collected from each tank were preserved in 70% ethanol for later counting. Finally, we calculated the percentage of settled larvae per plate type (blank and *Ulvella*-covered) per treatment using the average of the two pseudo-replicates per tank (Eq. (3)).

$$\frac{\text{number of settled larvae}}{\text{total larvae}} \times 100 \quad (3)$$

One tank was lost for the pH-elevated and 17 °C treatment, resulting in 2 instead of 3 replicates for that treatment.

2.13. Statistical analyses

All statistical analyses were performed in R (version 4.0.5) and RStudio software (RStudio, Boston, United States). Differences in hatching success, percentage of swimming larvae, shell length, behavioral parameters, larval respiration rate, and larval settlement on *Ulvella*-covered plates were assessed using a two-way analysis of variance (ANOVA) with pH, temperature, and the interaction between pH and temperature as fixed factors. For all of the aforementioned parameters, for each sampling time, the data were averaged per tank (n = 12 in total). Subsequently, our replicates are tanks (not individual larvae). The normality of the residuals was verified with a Shapiro–Wilk's test, and the homogeneity of variances was tested using Levene's test. To study the effects of pH and temperature on the settlement rate on blank plates, we applied a Wilcoxon rank sum test with continuity correction due to the presence of many zero values, and because the normality of the residuals could not be verified. To study the interaction between pH and temperature, we used a four-treatment-level Kruskal-Wallis rank sum test followed by a post hoc Wilcoxon rank sum test with continuity correction. The p and F values of two-way ANOVA are presented in the results, unless otherwise indicated.

To assess the frequency of the morphological and developmental parameters, we performed a four-treatment-level (low pH - low temperature; low pH - high temperature; high pH - low temperature; high pH - high temperature) chi-squared ($\chi 2$) test to evaluate the effects of pH and temperature on larval phenotypes at 24 and 72 hpf.

3. Results

3.1. Carbonate chemistry and physicochemical characteristics of seawater

The mean seawater temperature, salinity, and carbonate chemistry parameters are presented in Table 2. The salinity was 35.18 ± 0.04 psu in all experimental tanks, and remained stable over the course of the experiment. A_T measured in the experimental tanks was 2364 ± 17 μEq kg^{-1} and remained stable over the course of the experiment and between experimental aquaria. The mean pH_T values were 7.95 ± 0.04 and 7.68 ± 0.12 for the high and low-pH treatments, respectively. The average temperatures were 17.40 ± 0.55 °C and 19.35 ± 0.53 °C for the low and high temperature treatments, respectively (means ± SD).

3.2. Hatching success

The larval hatching success did not differ by temperature, pH, or the interaction of the two ($p > 0.05$; Table S1).

3.3. Percentage of swimming larvae

At 24 hpf, 72 hpf and 96 hpf the percentage of swimming larvae was significantly lower at 19 °C than at 17 °C (24 hpf: $F_{1,8}$ = 19.92, p = 0.002, Fig. 4A; 72 hpf: $F_{1,8}$ = 5.52, p = 0.046, Fig. 4C; 96 hpf: $F_{1,8}$ = 13.47, p = 0.006, Fig. 4E). However, no pH effect (24 hpf: $F_{1,8}$ = 0.41, p = 0.539, Fig. 4A;72 hpf: $F_{1,8}$ = 3.11, p = 0.115, Fig. 4C; 96 hpf: $F_{1,8}$ = 0.04, p = 0.845, Fig. 4E) and no interaction between temperature and pH (24 hpf: $F_{1,8}$ = 0.09, p = 0.764, Fig. 4B; 72 hpf: $F_{1,8}$ = 0.29, p = 0.602; Fig. 4D; 96 hpf: $F_{1,8}$ = 0.3, p = 0.618; Fig. 4F) were found.

Table 2
Mean parameters of seawater carbonate chemistry during the experiment. Total-scale seawater pH (pH_T), temperature, salinity, and total alkalinity (A_T) were used to calculate the partial pressure of CO_2 (pCO_2; μatm), dissolved inorganic carbon (DIC; μmol kg^{-1} SW), HCO_3^-, CO_3^{2-}, aragonite saturation state (Ωar), and calcite saturation state (Ωcalc) using CO2SYS software. The pH_T and temperature values shown represent the average value for each treatment, measured daily over the 5 days of the experiment (n = 15 per treatment). Salinity was measured once a day over the 5 days of the experiment (n = 5 per treatment). Results are expressed as mean ± SD.

Treatment name	Treatment (pH-T°C)	Temperature (°C)	pH_T	pCO_2 (μatm)	DIC	HCO_3^- (μmol · kg^{-1})	CO_3^{2-} (μmol · kg^{-1})	Ωar	Ωcalc
High pH – low temperature	8.0–17 °C	17.5 ± 0.6	7.99 ± 0.04	478 ± 49	2122 ± 16	1950 ± 24	156 ± 10	2.40 ± 0.15	3.72 ± 0.23
Low pH – high temperature	7.7–19 °C	19.4 ± 0.6	7.66 ± 0.12	1161 ± 319	2245 ± 45	2118 ± 58	88 ± 24	1.36 ± 0.37	2.10 ± 0.56
High pH – high temperature	8.0–19 °C	19.3 ± 0.5	7.91 ± 0.05	593 ± 74	2147 ± 23	1985 ± 35	142 ± 14	2.20 ± 0.22	3.39 ± 0.34
Low pH – low temperature	7.7–17 °C	17.3 ± 0.5	7.71 ± 0.11	999 ± 263	2236 ± 39	2109 ± 51	91 ± 21	1.40 ± 0.32	2.173 ± 0.49

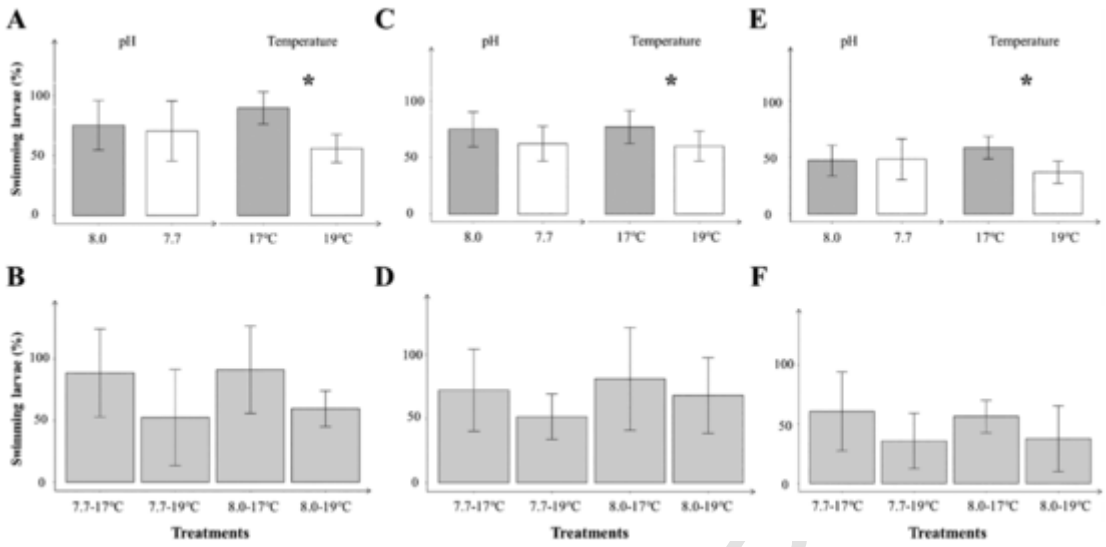

Fig. 4. Effects of pH and temperature on *Haliotis tuberculata* percentage of swimming larvae at A) 24 h post-fertilization (hpf), C) 72 hpf, and E) 96 hpf (n = 6 tanks per treatment). Combined treatment effects of pH and temperature on *H. tuberculata* percent swimming larvae at B) 24 hpf, D) 72 hpf, and F) 96 hpf (n = 3 tanks per treatment). Bar values represent means and error bars represent the standard deviation of the mean. Asterisks denote significant differences between temperature treatments by two-way ANOVA.

3.4. Morphometric characteristics

3.4.1. 24 hpf larvae

Shell formation was significantly affected by temperature (X^2 (2) = 54.59, $p < 0.001$), pH (X^2 (2) = 94.82, $p < 0.001$), and the four treatment levels (low pH - low temperature, low pH - high temperature, high pH - low temperature, high pH - high temperature); (X^2 (6) = 130.71, $p < 0.001$) (Fig. 5A; Table S2). Larvae exposed to pH 7.7 were 4.5 times less likely to have normal shell formation compared with larvae exposed to pH 8.0 (9.9% at pH 7.7 versus 45% at pH 8.0; Table S2). Larvae exposed to 19 °C temperatures were 3 times as likely to have normal shell formation compared with larvae exposed to 17 °C temperatures (45% at 19 °C versus 15% at 17 °C; Table S2). The larvae exposed to the low pH and low temperature treatment had

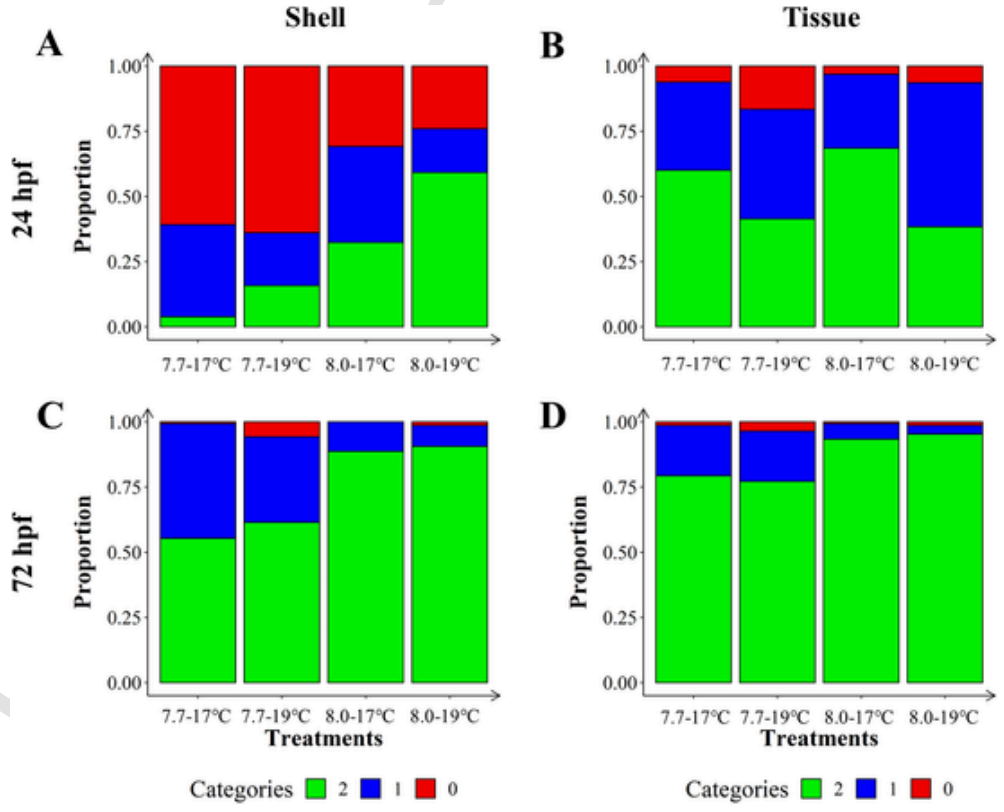

Fig. 5. Proportional distribution of larvae at 24 h post-fertilization (hpf) (A and B) and at 72 hpf (C and D) according to their morphological categories. Colored bars indicate the degree of malformation for each variable. A and C: shell formation score (2 = normal shell; 1 = partially and/or abnormally developed shell; 0 = no shell). B and D: tissue organogenesis score (2 = normally developed tissues; 1 = partially or abnormally developed tissues; 0 = undeveloped tissues). The frequencies of each category are shown (n = 518 larvae in total).

the lowest proportion of normal shell formation, whereas larvae exposed to the high pH and high temperature treatment had the highest proportion of normal shell formation (4% vs 59%, respectively) (Fig. 5A; Table S2).

Similarly, tissue organogenesis at 24 hpf was significantly affected by temperature (X^2 (2) = 24.75, $p < 0.001$), pH (X^2 (2) = 7.83, $p = 0.020$), and the four treatment levels (low pH - low temperature, low pH - high temperature, high pH - low temperature, high pH - high temperature); (X^2 (6) = 45.46, $p < 0.001$) (Fig. 5B; Table S2). Larvae exposed to the high temperature had a lower proportion of normally developed tissues than did larvae exposed to the low temperature (39% at 19 °C versus 61% at 17 °C; Table S2), whereas larvae exposed to both low-pH and high pH conditions had similar tissue organogenesis (51% at pH 7.7 versus 54% pH 8.0).

3.4.2. 72 h larvae

Shell formation was significantly affected by temperature (X^2 (2) = 10.61, $p = 0.005$), pH (X^2 (2) = 71.19, $p < 0.001$), and the four treatment levels (low pH - low temperature, low pH - high temperature, high pH - low temperature, high pH - high temperature; X^2 (6) = 84.76, $p < 0.001$) (Fig. 5C; Table S2). Larvae exposed to pH 7.7 had a significantly lower proportion of specimens with normal shell development compared with larvae exposed to the high pH of 8.0 (60% at pH 7.7 versus 90% at pH 8.0) (Fig. 5C; Table S2). The larvae in the high pH and high temperature treatment showed the highest proportion of specimens with normal shell development (92%), followed by those in the high pH and low temperature treatment (88%). Larvae exposed to the low-pH and low temperature treatment had the lowest proportion of specimens with normal shell development (56%; Fig. 5C; Table S2).

Tissue organogenesis at 72 hpf was significantly affected by pH (X^2 (2) = 36.15, $p < 0.001$) and by the four treatment levels (low pH - low temperature, low pH - high temperature, high pH - low temperature, high pH - high temperature; X^2 (6) = 39.54, $p < 0.001$) (Fig. 5D; Table S1), but was not significantly affected by temperature (X^2 (2) = 2.70, $p = 0.26$). Larvae exposed to the low-pH had a significantly lower proportion of specimens with normally developed tissues (78%) compared with larvae exposed to the high pH (95%; Table S2).

3.5. Shell length

The shell length of the 24-hpf larvae could not be measured in the low-pH treatments because there were very few larvae with normally developed shells (Fig. 5A). The shell length of the 72-hpf larvae was significantly shorter in the low-pH treatments compared with the high pH treatments ($F_{1,8}$ = 11.90, p = 0.008; pH 8.0$_{mean}$ = 265.01 ± 6.69 μm; pH 7.7$_{mean}$ = 258.57 ± 10.61 μm). However, the temperature had no effect on larval shell length at 72 hpf ($F_{1,8}$ = 4.66, p = 0.063; 17 °C$_{mean}$ = 264.83 ± 8.49 μm; 19°C$_{mean}$ = 260.28 ± 8.89 μm). No interaction between temperature and pH was observed ($F_{1,8}$ = 1.60, p = 0.24; 8.0–17 °C$_{mean}$ = 265.92 ± 6.92 μm; 8.0–19 °C$_{mean}$ = 264.09 ± 6.34 μm; 7.7–17 °C$_{mean}$ = 263.00 ± 10.38 μm; 7.7–19 °C$_{mean}$ = 254.44 ± 9.09 μm).

3.6. Shell calcification

The mean birefringence (number of grayscale pixels) at 24 hpf was significantly lower at pH 7.7 than at the high pH of 8.0 ($F_{1,8}$ = 8.55, p = 0.019; Fig. 6A). However, birefringence (and correspondingly, shell calcification) did not differ significantly by temperature ($F_{1,8}$ = 1.33, p = 0.281; Fig. 6A) or by the interaction between temperature and pH ($F_{1,8}$ = 0.01, p = 0.920; Fig. 6B). The mean birefringence at 72 hpf was significantly lower in the pH 7.7 compared with pH 8.0

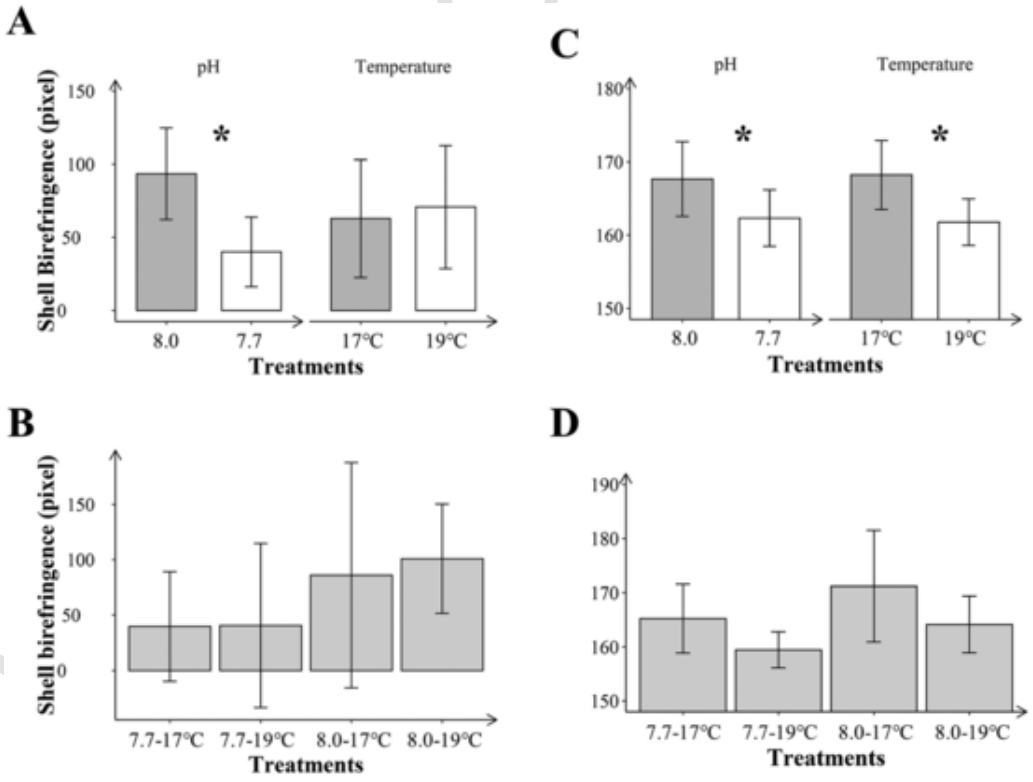

Fig. 6. Individual effects of pH and temperature on mean shell birefringence of larvae at A) 24 hpf and C) 72 hpf (n = 6 tanks per treatment). Combined effects of pH and temperature on mean shell birefringence of larvae at B) 24 hpf and D) 72 hpf (n = 3 tanks per treatment). Bar values represent means and error bars represent the standard deviation of the mean. Asterisks indicate significant differences between either temperature or pH treatments, as determined by two-way ANOVA.

($F_{1,8}$ = 12.21, p = 0.008) and 19 °C compared with 17 °C ($F_{1,8}$ = 17.83, p = 0.003) treatments, indicating reduced shell calcification in low pH treatment and high temperature treatment compared with the ambient pH and temperature respectively (Fig. 6C). However, the interaction between temperature and pH did not significantly affect shell birefringence at 72 hpf ($F_{1,8}$ = 0.08, p = 0.784; Fig. 6D).

3.7. Scanning electron microscopy

In the high pH treatments (8.0), the shell surface of larvae observed at 24 hpf showed a normal granular texture with an alveolar pattern (Fig. 7A, B, E, F). However, the larvae reared in the low-pH treatments (7.7) showed signs of shell deformation and microfractures (Fig. 7C, D). Details of the shell surface boxed in Fig. 7C and D revealed irregularities and mineralization defects that were probably due to shell dissolution. The shell surface of larvae observed at 72 hpf were of similar

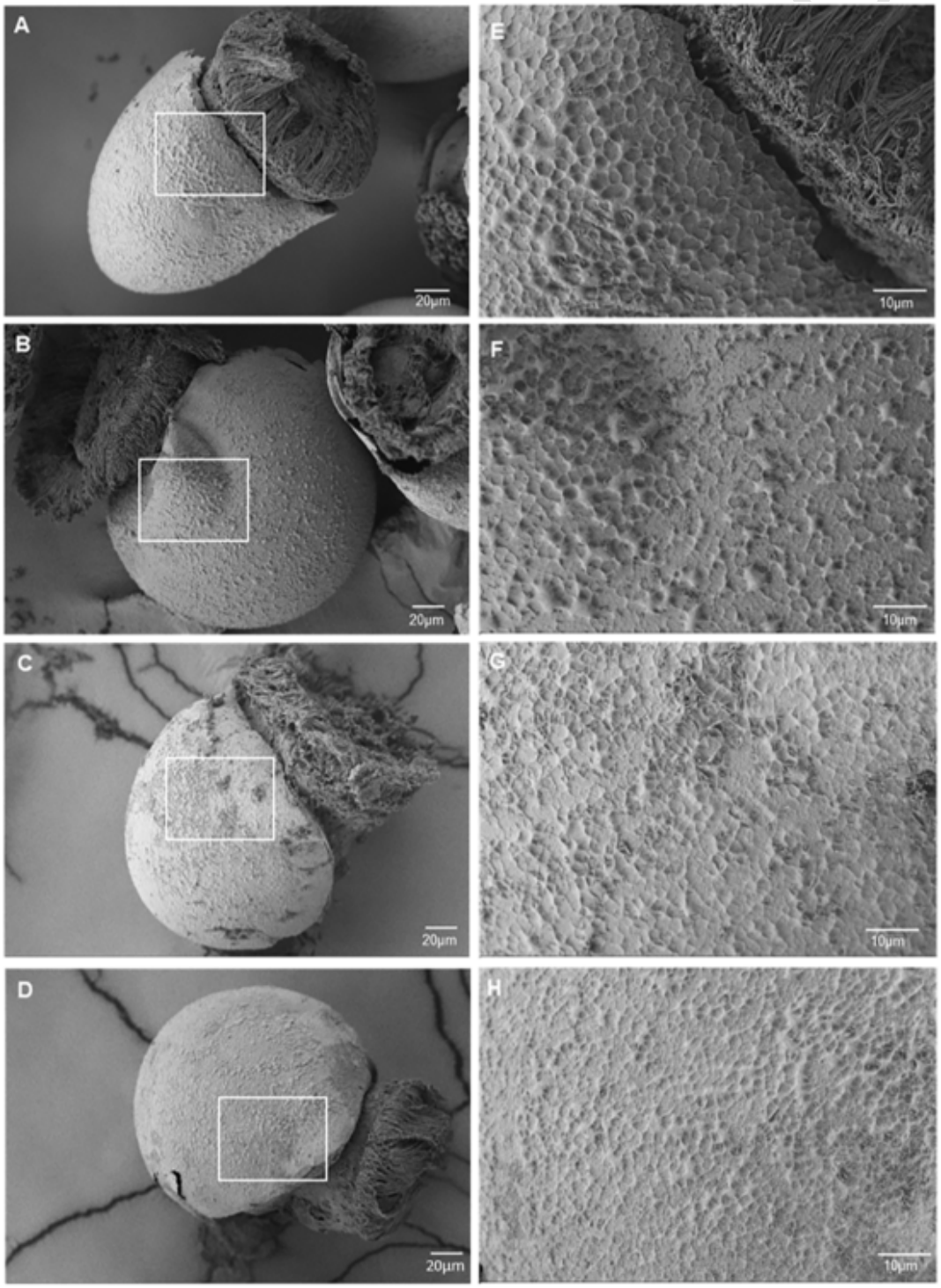

Fig. 7. Scanning electron microscopy (SEM) images of *Haliotis tuberculata* larvae at 24 hpf in the four experimental treatments A) pH 8.0–17 °C; B) pH 8.0–19 °C; C) pH 7.7–17 °C; and D) pH 7.7–19 °C. Lateral views of the larvae show the protoconch shell and the velum. E–H show magnified views of the corresponding white squares in A–D.

shape and pattern in both the low (7.7) and high (8.0) pH treatments (Fig. 8A–D). At higher magnification, the shell surfaces of high pH larvae revealed a homogeneous granular texture and alveolar pattern (Fig. 8E, F). In the low-pH treatments, the details of the shell surface boxed in Fig. 8C and D revealed surface heterogeneities and small holes within the alveolar network suggesting mineral dissolution. (Fig. 8G, H).

The shell surface of larvae observed at 72 hpf were of similar shape and pattern in both the low (7.7) and high (8.0) pH treatments (Fig. 8A–D). The magnified areas of the shells in all treatments revealed a typical granular texture and alveolar pattern (Fig. 8E–H). However, the surface heterogeneities and small holes within the alveolar network in the low-pH treatments (Fig. 8G, H) suggest mineral dissolution.

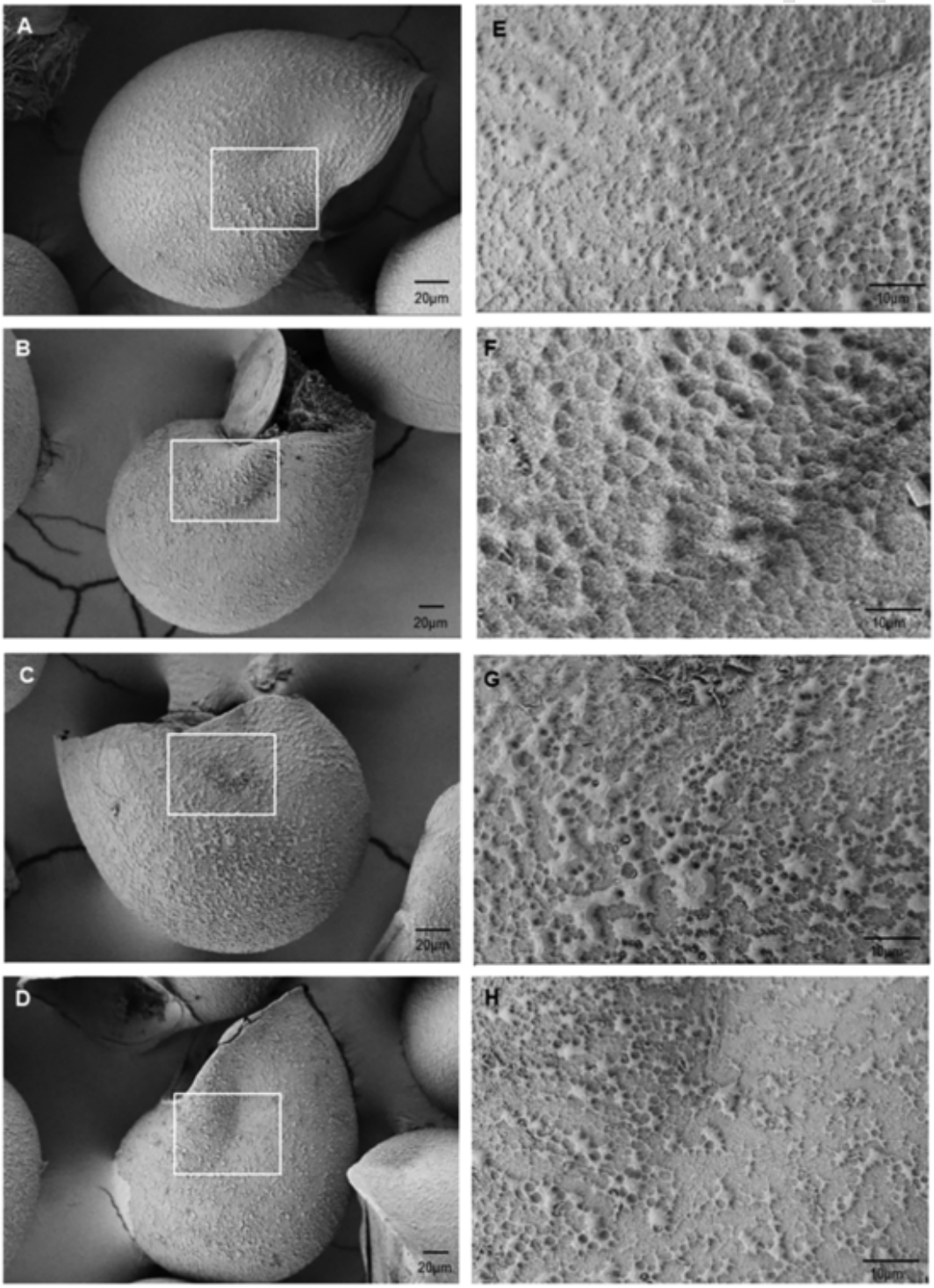

Fig. 8. Scanning electron microscopy (SEM) images of *Haliotis tuberculata* larvae at 72 hpf in the four experimental treatments A) pH 8.0–17 °C; B) pH 8.0–19 °C; C) pH 7.7–17 °C; and D) pH 7.7–19 °C. Lateral views of the larvae show the well-developed protoconch covering the larval body. In A, the protoconch is well developed and covers the larval body. In B, the operculum closes the shell aperture after complete retraction of the veliger. E–H show magnified views of the corresponding white squares in A–D.

3.8. Larval swimming behavior

None of the larval behavioral parameters - distance moved (total mm^{-1})), mean velocity ($mm \cdot s^{-1}$), and mean meander ($deg \cdot mm^{-1}$) - differed significantly due to pH, temperature, or the interaction between pH and temperature (Table S3).

3.9. Respiration rate

The respiration rate of larvae did not differ significantly between pH ($F_{1,8}$ = 0.66, p = 0.440; two-way ANOVA), or temperature ($F_{1,8}$ = 4.06, p = 0.078; two-way ANOVA). In addition, No interaction was found between pH and temperature ($F_{1,8}$ = 2.20, p = 0.176).

3.10. Larval settlement

The larval settlement on *Ulvella*-covered plates was significantly higher in the high temperature (19 °C) treatments than in the low temperature (17 °C) treatments ($F_{1,7}$ = 14.02, p = 0.007; Fig. 9A). No significant differences were observed between pH treatments ($F_{1,7}$ = 1.40, p = 0.275; Fig. 9A) or from the interaction between pH and temperature ($F_{1,7}$ = 0.47, p = 0.52; Fig. 9C).

On blank plates, we found significant effects from temperature (W = 0, p = 0.005; Wilcoxon rank sum test with continuity correction; Fig. 9C) and from the four treatment comparisons (H (3) = 8.70, p = 0.033; Kruskal–Wallis) (Fig. 9D). Larval settlement on the blank plates was significantly higher in the high temperature (19 °C) treatments than in the low temperature (17 °C) treatments (Fig. 9B). No significant differences were found between the low-pH and high pH treatments (W = 14, p = 0.923; Wilcoxon rank sum test with continuity correction; Fig. 9C).

4. Discussion

In this study, we exposed *H. tuberculata* larvae to the individual and combined effects of OA and OW. We found that a 0.3-unit decrease in pH and a 2 °C increase in temperature caused broad effectson the responses of the larvae (Table 3). However, no significant interactive effects of temperature and pH were observed for the variables measured. Among the biological parameters investigated in this study, shell formation, length, and calcification appeared to be the most sensitive to the effects of temperature and pH. The results of this study lend further support to the results from recent meta-analyses suggesting that the interactive effects of OA and OW on calcifying species, including mollusks, are not as ubiquitous as OA's and OW's individual effects (Kroeker et al., 2013; Przeslawski et al., 2015).

The hatching success of trochophore larvae of *H. tuberculata* was not significantly affected by temperature, pH, or the interaction of the two. These results are in line with those of Pedroso (2017), who found no impact on the hatching success of *Haliotis asinina* in response to raising the ambient temperature of 29 °C by 2 °C. The lack of significant effects by pH or by the interaction of pH and temperature was likewise similar to previous findings. Guo et al. (2015) found no effect of pH_{NBS} 7.94 on the hatching success of *H. diversicolor* and *Haliotis discus*, whereas both species experienced reduced hatching success when the pH value was decreased to 7.71 or lower, compared with the high pH of 8.15. In two separate studies on the hatching success of *Haliotis discus hannai*, Kimura et al. (2011) and Li et al. (2013) found no impact of exposure to pH_{NBS} 7.6 and higher, compared with pH of 8.02. Likewise, Tahil and Dy (2016) found that pH_{NBS} 7.78 did not affect the *H. asinina* hatching success compared to the pH of 7.97; however, pH treatments of 7.60 and 7.40 negatively affected the hatching success. Our results show that *H. tuberculata* larvae can hatch at the lower pH values and high temperatures expected in the coming decades. Such tolerance to OA and OW in

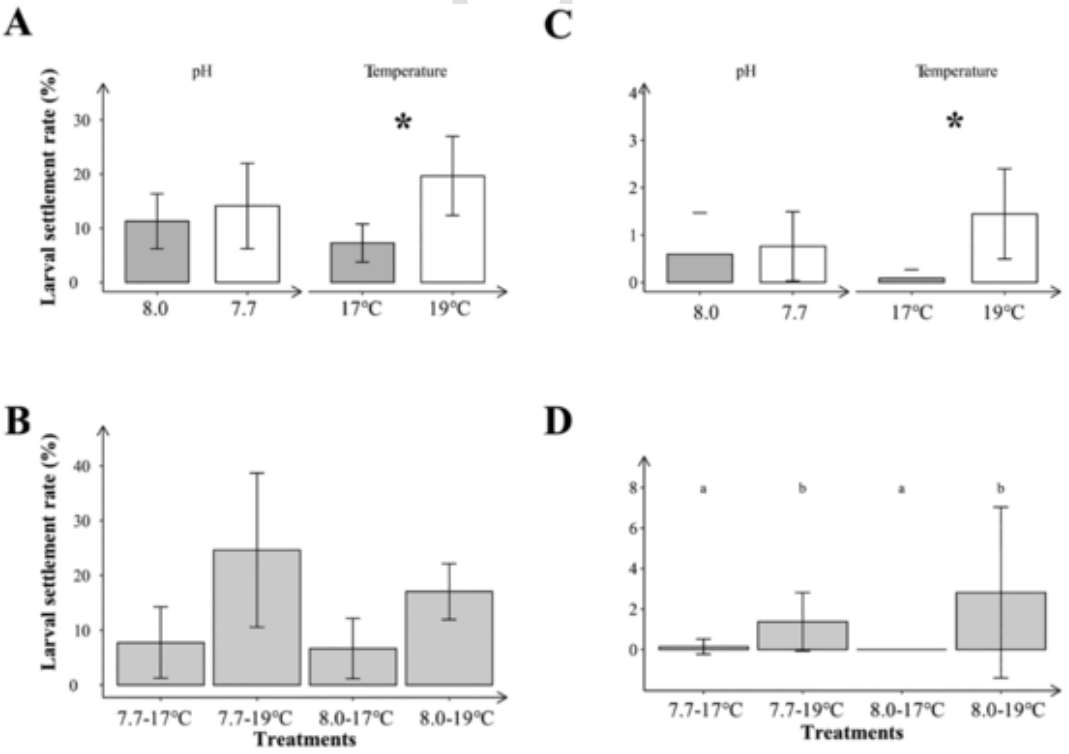

Fig. 9. Effects of pH and temperature on larval settlement on A) plates covered with the green microalga *Ulvella lens* (n = 6 tanks per treatment; two-way ANOVA) and B) blank plates (n = 6 tanks per treatment; Wilcoxon rank sum test with continuity correction). Combined effects of pH and temperature on larval settlement on C) *Ulvella*-covered plates and D) blank plates at 96 h post-fertilization (hpf) (n = 3 tanks per treatment). Bar values represent means and error bars represent the standard deviation of the mean. Different lowercase letters indicate significant differences among treatments. Asterisks indicate significant differences between either temperature or pH treatments. (For interpretation of the references to colour in this figure legend, the reader is referred to the web version of this article.)

Table 3
Full results summary showing the effects of temperature, pH, and their interaction on the various parameters observed during this study. Arrow direction indicates whether these factors decreased/diminished (↓), increased/enhanced (↑), or had no significant effect (ns) on the measured parameters of *H. tuberculata* at 24, 72, and 96 h post-fertilization (hpf). Empty cells indicate that the corresponding results were not applicable because they were not measured. Where non-parametric tests were used (i.e., for shell formation and tissue formation), treatment impacts are shown instead of interaction effects.

Parameter	Temperature effect			pH effect			Interaction effect		
	24 hpf	72 hpf	96 hpf	24 hpf	72 hpf	96 hpf	24 hpf	72 hpf	96 hpf
Hatching success	ns			ns			ns		
Percentage of swimming larvae	↓	↓	↓	ns	ns	ns	ns	ns	ns
Shell formation	↑	↓		↓	↓		8.0–17 °C = ambient 7.7–19 °C = ↓ 8.0–19 °C = ↑ 7.7–17 °C = ↓	8.0–17 °C = ambient 7.7–19 °C = ↓ 8.0–19 °C = ns 7.7–17 °C = ↓	
Tissue formation	↓	ns		↓	↓		8.0–17 °C = ambient 7.7–19 °C = ↓ 8.0–19 °C = ↓ 7.7–17 °C = ns	8.0–17 °C = ambient 7.7–19 °C = ↓ 8.0–19 °C = ns 7.7–17 °C = ↓	
Shell length		ns			↓			ns	
Shell calcification	ns	↓		↓	↓		ns	ns	
Respiration rate		ns			ns			ns	
Larval swimming behavior		ns			ns			ns	
Larval settlement			↑			ns			ns

the early larval stages has already been reported for other marine species (Przeslawski et al., 2015), and might originate from protective factors in the egg (Hamdoun and Epel, 2007).

An increased number of larvae with tissue abnormalities was observed under high temperature treatments. This was accompanied by significant declines in the percentage of swimming larvae in the high temperature treatments compared to the low temperature treatments at 24, 72 and 96 hpf. Low pH, also, reduced the normal tissue development of the larval stages. A study on *H. asinina* found <1% of normal trochophores at the reduced pH of 7.60, compared with the ambient pH of 7.97 (Tahil and Dy, 2016). Parker et al. (2012) also reported slower larval development in the Sydney rock oyster, *Saccostrea glomerata*, when the ambient pH (pH_{NBS} 8.2) was reduced by 0.3 pH units. A study by Wessel et al. (2018) on *H. tuberculata* showed a significant increase in the number of 30-hpf larvae with abnormal and delayed development at pH_T 8.0 compared with larvae at pH_T 7.7 and 7.6. These findings suggest that a difference of only a few hours of exposure to stressors can influence their effects during larval development.

Larval shell formation was also impaired under low pH, similar to previous studies on *Haliotis coccoradiata* (pH_{NBS} = 7.8 and 7.6 compared with the ambient pH of 8.2; Byrne et al., 2011); *Haliotis kamtschatkana* (reported as pCO_2 values of 800 µatm and 1800 µatm compared with a control of 400 µatm; Crim et al., 2011); *H. asinina* (pH_{NBS} = 7.85 and 7.65 compared with the ambient pH of 8.15; Santander, 2018); and *H. tuberculata* (pH_T = 7.68 and 7.58 compared with the ambient pH of 8.00; Wessel et al., 2018). Shell calcification of *H. tuberculata* larvae was also reduced under low pH, as shown by the decrease in birefringence intensity measured at 24 and 72 hpf. Additional SEM observations revealed differences in larval shell texture and the presence of numerous small holes on the outer shell surface, suggesting that $CaCO_3$ dissolution may be responsible for the reduced calcification seen in larvae raised at a lower pH. The lack of calcification observed under cross-polarization microscopy and SEM is consistent with previous results from Wessel et al. (2018), and provides further evidence that abalone larvae deposit less $CaCO_3$ and produce more fragile and thinner shells when exposed to OA. Our results confirm, as reported for numerous mollusk species, that the growing calcified shells of larval and juvenile abalones are highly sensitive to OA (Gazeau et al., 2013; Przeslawski et al., 2015). Naturally occurring *H. tuberculata* populations may be at greater risk from future pH reduction, as early shell alterations may impair larval development and recruitment.

In this study, the impaired process of shell formation induced by low pH was mitigated by high temperature, resulting in a higher proportion of 24- and 72-hpf larvae with normal shell development as shown in Fig. 5A and C. Observations of temperature reducing the negative impacts of OA on shell calcification and development have been previously reported for larval and juvenile mollusks (Davis et al., 2013; Ko et al., 2014).

Shell length of *H. tuberculata* larvae was significantly reduced by low-pH conditions, but no temperature or interaction effects were observed. Crim et al. (2011) reported a 5% reduction in larval shell size in the northern abalone *H. kamtschatkana* after an 8-day exposure to acidified conditions (reported as CO_2 levels 400 µatm vs 800 µatm), which is consistent with our results (4% reduction at 24 hpf and 6% reduction at 72 hpf). Similarly, the larvae of *H. asinina* (pH_{NBS} = 7.85 and 7.65 compared with the ambient pH of 8.15; Santander, 2018); *H. diversicolor*; and *H. discus hannai* (pH_{NBS} = 7.94 and lower compared with the high pH of 8.15; Guo et al., 2015) experienced reductions in shell length at low-pH compared with high pH conditions. In a study by Onitsuka et al. (2018), larvae of *H. discus hannai* at pH_{NBS} 7.79 did not show any significant reduction in shell length compared with larvae at the high pH_{NBS} of 7.99.

In our study, the lack of significant effects on shell size from temperature or from the interaction between temperature and pH is consistent with results obtained for other marine mollusks. For example, Thiyagarajan and Ko (2012) reported no impact of high temperature (30 °C compared with 24 °C), or temperature–pH interaction on the shell size of the Portuguese oyster *Crassostrea angulata*. On the other hand, Talmage and Gobler (2011) recorded decreased larval size in two bivalves (*Mercenaria mercenaria* and *Argopecten irradians*) resulting from both a reduced pH_{NBS} of 7.8 (compared with the ambient pH of 8.08) and an high temperature of 28 °C (compared with the ambient temperature of 24 °C). These contrasting effects confirm a high variability in the responses of marine mollusk larvae to both isolated and combined stressors.

The absence of direct effects of pH and temperature on larval physiology and behavior does not rule out the existence of their indirect effects through cellular and molecular mechanisms that were not measured in the present study. Indeed, larval developmental stages are characterized by huge changes (in physiology and sensitivity) over a short period of time (5 days) and the measurements of physiological and behavioral variables do not account for the whole developmental processes that may be impacted by the stressors. Complementary studies at the molecular level (i.e., gene expression, protein and enzyme synthesis, etc.) will be needed to fully understand the fine developmental changes induced by the climate change drivers (Pörtner, 2010).

Larval settlement was greater at high temperatures than at the low temperature on both *Ulvella*-covered and blank plates. The shorter lar-

val duration that corresponded with high temperature in this study is consistent with previous studies of related *Haliotis* species, such as *H. sorenseni*, *H. rufescens*, *H. corrugata*, and *H. fulgens* (Leighton, 1972, 1974). This suggests that high temperatures resulting from global warming reduce the duration of the planktonic larval stage and accelerate the settlement rate (Byrne et al., 2011). This may be an advantage (Byrne et al., 2011), as a longer planktonic stage may reduce the chances of survival due to increased risk of predation and exposure to other environmental stresses (Parker et al., 2013). We did not record any significant effects of pH on *H. tuberculata* settlement, which is in line with the findings of another study on *H. kamtschatkana* (Crim et al., 2011). However, the literature contains contradictory results, with a tendency toward a lower settlement rate of the New Zealand abalone, *H. iris*, in low-pH conditions (Espinel-Velasco et al., 2021) as well as for the donkey's ear abalone, *H. asinina*, in three low-pH treatments (Tahil and Dy, 2015).

Our results showed that in every treatment, the settlement rate of *H. tuberculata* larvae on *Ulvella*-covered plates was higher than the settlement rate on blank plates by a factor of at least 15. This supports the notion that settlement cues increase marine invertebrate larval settlement (Hadfield and Paul, 2001; Pawlik, 1992; Rodriguez et al., 1993). However, lowered pH may cause indirect effects, due to the effect of low pH on the settlement substrate. For example, O'Leary et al. (2017) reported that the settlement rate of *H. rufescens* under both present-day and low-pH treatments increased from 11% in tanks with no crustose coralline algae, to ~70% in the presence of crustose coralline algae. This raises another concern regarding the indirect impacts of OA and OW on abalone larval settlement. Coralline algae are common settlement cues for abalone larvae (De Viçose et al., 2010, 2012; Williams et al., 2008; Roberts et al., 2004; Roberts and Nicholson, 1997), and they are decreasing due to OA and OW (Kuffner et al., 2008; Martin and Gattuso, 2009; Diaz-Pulido et al., 2011; Hofmann et al., 2012). Therefore, even in the absence of the direct impacts of OA and OW on abalone larvae, such environmental changes may indirectly reduce larval settlement by reducing their settlement cues. On the other hand, if *Ulvella* species, like many non-calcifying macroalgae, can benefit from high temperatures and reduced pH (Koch et al., 2012; Hofmann et al., 2012), then abalone larvae may be able to maintain their normal settlement rates. This presents an area requiring further examination.

None of the other behavioral responses (distance moved (total mm^{-1}), mean velocity ($mm \cdot s^{-1}$), mean meander ($deg \cdot mm^{-1}$)) differed as an effect of pH, temperature, or the interaction between the two. These outcomes parallel the responses of 2-day-old larvae of the Pacific oyster, *Crassostrea gigas*, when exposed to high pH and low (−0.3 units) pH conditions (Valentini, 2019). Although the method used in this research to study larval behavior is very common, it is noted that applying such a two-dimensional method may not allow the abalone larvae to express natural swimming behavior. Therefore, developing three dimensional methods are desired for future studies.

The lack of significant changes in larval behavior may partly justify the lack of changes observed in larval respiration. Larval respiration of *H. tuberculata* did not differ due to the individual or combined factors of pH and temperature. Although very low pH and highly high temperatures (i.e., out of the projected ranges for the year 2100) are known to amplify respiration (Campanati et al., 2018; Waldbusser et al., 2015; Liu and He, 2012; Padilla-Gamiño et al., 2013), some studies have confirmed that respiration was not impacted by a −0.3 unit pH reduction and/or a + 3 °C temperature increase above the ambient conditions (Frieder et al., 2016). For example, the respiration rate of the larvae of *Mytilus californianus* did not change when the ambient pH was reduced from 8.3 to 7.8 (Waldbusser et al., 2015). Similarly, Campanati et al. (2018) found no impact on the oxygen consumption of *Reishia clavigera* larvae when the ambient pH was reduced from 8.1 to 7.6. High pCO_2 in seawater likely increases the maintenance costs of acid–base homeostasis, the intracellular ion balance required for protein folding and pH-sensitive physiological processes (Rivest and Hofmann, 2014; Lefevre, 2016). Therefore, our observation in this study of a lack of increase in *H. tuberculata* metabolic rates under acidified conditions may suggest that the larvae were able to use existing pools of ion pumps to conserve their acid–base homeostasis (Portner and Reipschlager, 1996; Guppy and Withers, 1999).

In conclusion, the majority of the responses of *H. tuberculata* larvae were affected by low pH and high temperature, but not by their interactions as summarized in Table 3. . Even though the projected rates of pH decrease and temperature increase over the coming decades may not seem to be an obstacle for *H. tuberculata* larval production, it seems that under OA and OW, the majority of this species' responses are susceptible to changes in either temperature or pH. Thus, *H. tuberculata* larvae will have to cope with both stressors. In nature, this may happen through physiological adaptation / acclimatization or via natural climate change refugia. In abalone farms, this can occur using various strategies. For example, by monitoring of the daily changes in seawater pH, it can be arranged to avoid pumping low pH seawater into the farms during the hours when the CO_2 concentrations in the seawater is at its peak ion (Murie and Bourdeau 2020). If farms have access to large-volume storage tanks, adding kelp species to the tanks may reduce CO_2 concentrations as kelp canopies have the ability to alter local seawater chemistry (Murie and Bourdeau 2020). Inclusion of an integrated multi-trophic aquaculture system based on algae might be helpful (Bolton et al. 2009). Adding chemicals to increase seawater alkalinity and/or pH might be another solution for the hatcheries with a recirculating system. The selection of tolerant broodstocks to OA and GW can be also undertaken.

Huchette, 2004

Parker et al., 2012

CRediT authorship contribution statement

Javid Kavousi: Conceptualization, Methodology, Investigation, Formal analysis, Writing – original draft, Writing – review & editing, Visualization. **Sabine Roussel:** Conceptualization, Methodology, Investigation, Formal analysis, Writing – review & editing, Visualization, Supervision. **Sophie Martin:** Conceptualization, Methodology, Investigation, Writing – review & editing. **Fanny Gaillard:** Conceptualization, Methodology, Investigation. **Aicha Badou:** Conceptualization, Methodology, Investigation. **Carole Di Poi:** Conceptualization, Methodology, Investigation, Writing – review & editing. **Sylvain Huchette:** Conceptualization, Methodology, Investigation. **Philippe Dubois:** Conceptualization, Writing – review & editing. **Stéphanie Auzoux-Bordenave:** Conceptualization, Methodology, Investigation, Formal analysis, Writing – review & editing, Visualization, Supervision.

Declaration of competing interest

No conflict of interest exists.

Acknowledgements

JK was supported by a post-doctoral fellowship from the French government under the program “Investissements d'Avenir”, co-funded by the ISblue project “Interdisciplinary graduate school for the blue planet” (ANR-17-EURE-0015). This work was supported in part by the program “Acidification des Océans” (ICOBio project) funded by the Fondation pour la Recherche sur la Biodiversité (FRB) and the Ministère de la Transition Ecologique et Solidaire (MTES). The Regional Council of Brittany, the General Council of Finistère, the urban community of Concarneau Cornouaille Agglomération and the European Regional De-

velopment Fund (ERDF) are acknowledged for the funding of the scanning electron microscope (Sigma 300 FE-SEM) at the Concarneau Marine Station. Philippe Dubois is a Research Director of the National Fund for Scientific Research (Belgium). We thank Stéphane Formosa for his assistance in SEM (Plateau technique de Microscopie Electronique du Muséum National d'Histoire Naturelle, Concarneau, France). We thank all the staff of the France Haliotis farm (Plouguerneau) for hosting the experiment.

Appendix A. Supplementary data

Supplementary data to this article can be found online at https://doi.org/10.1016/j.marpolbul.2021.113131.

References

Auzoux-Bordenave, S., Badou, A., Gaume, B., Berland, S., Helléouet, M.-N., Milet, C., Huchette, S., 2010. Ultrastructure, chemistry and mineralogy of the growing shell of the European abalone Haliotis tuberculata. J. Struct. Biol. 171, 277–290.

Auzoux-Bordenave, S., Wessel, N., Badou, A., Martin, S., M'zoudi, S., Avignon, S., Roussel, S., Huchette, S., Dubois, P., 2020. Ocean acidification impacts growth and shell mineralization in juvenile abalone (Haliotis tuberculata). Mar. Biol. 167, 1–14.

Avignon, S., Auzoux-Bordenave, S., Martin, S., Dubois, P., Badou, A., Coheleach, M., Richard, N., Di Giglio, S., Malet, L., Servili, A., 2020. An integrated investigation of the effects of ocean acidification on adult abalone (Haliotis tuberculata). ICES J. Mar. Sci. 77, 757–772.

Bolton, J.J., Robertson-Andersson, D.V., Shuuluka, D., Kandjengo, L., 2009. Growing ulva (Chlorophyta) in integrated systems as a commercial crop for abalone feed in South Africa: a SWOT analysis. J. Appl. Phycol. 21, 575–583.

Byrne, M., Ho, M., Wong, E., Soars, N.A., Selvakumaraswamy, P., Shepard-Brennand, H., Dworjanyn, S.A., Davis, A.R., 2011. Unshelled abalone and corrupted urchins: development of marine calcifiers in a changing ocean. Proc. Biol. Sci. 278, 2376–2383. https://doi.org/10.1098/rspb.2010.2404.

Campanati, C., Dupont, S., Williams, G.A., Thiyagarajan, V., 2018. Differential sensitivity of larvae to ocean acidification in two interacting mollusc species. Mar. Environ. Res. 141, 66–74. https://doi.org/10.1016/j.marenvres.2018.08.005.

Cook, P.A., 2016. Recent trends in worldwide abalone production. J. Shellfish Res. 35, 581–583.

Crim, R.N., Sunday, J.M., Harley, C.D.G., 2011. Elevated seawater CO2 concentrations impair larval development and reduce larval survival in endangered northern abalone (Haliotis kamtschatkana). J. Exp. Mar. Biol. Ecol. 400, 272–277. https://doi.org/10.1016/j.jembe.2011.02.002.

D'Amario, B., Pérez, C., Grelaud, M., Pitta, P., Krasakopoulou, E., Ziveri, P., 2020. Coccolithophore community response to ocean acidification and warming in the Eastern Mediterranean Sea: results from a mesocosm experiment. Sci. Rep. 10, 1–14.

Daume, S., Brand-Gardner, S., Woelkerling, W.J., 1999. Preferential settlement of abalone larvae: diatom films vs. non-geniculate coralline red algae. Aquaculture 174, 243–254. https://doi.org/10.1016/s0044-8486(99)00003-4.

Daume, S., Huchette, S., Ryan, S., Day, R.W., 2004. Nursery culture of Haliotis rubra: the effect of cultured algae and larval density on settlement and juvenile production. Aquaculture 236, 221–239. https://doi.org/10.1016/j.aquaculture.2003.09.035.

Davis, A.R., Coleman, D., Broad, A., Byrne, M., Dworjanyn, S.A., Przeslawski, R., 2013. Complex responses of intertidal molluscan embryos to a warming and acidifying ocean in the presence of UV radiation. PLoS One 8, e55939. https://doi.org/10.1371/journal.pone.0055939.

De Viçose, G.C., Viera, M.P., Huchette, S., Izquierdo, M.S., 2012. Larval settlement, early growth and survival of Haliotis tuberculata coccinea using several algal cues. J. Shellfish Res. 31, 1189–1198. https://doi.org/10.2983/035.031.0430.

Di Santo, V., 2015. Ocean acidification exacerbates the impacts of global warming on embryonic little skate, Leucoraja erinacea (Mitchill). J. Exp. Mar. Biol. Ecol. 463, 72–78.

Diaz-Pulido, G., Anthony, K.R.N., Kline, D.I., Dove, S., Hoegh-Guldberg, O., 2011. Interactions between ocean acidification and warming on the mortality and dissolution of coralline algae1. J. Phycol. 48, 32–39. https://doi.org/10.1111/j.1529-8817.2011.01084.x.

Dickson, A.G., Millero, F.J., 1987. A comparison of the equilibrium constants for the dissociation of carbonic acid in seawater media. Deep Sea research part aOceanographic Research Papers 34, 1733–1743. https://doi.org/10.1016/0198-0149(87)90021-5.

Dickson, A.G., Sabine, C.L., Christian, J.R., 2007. Guide to Best Practices for Ocean CO2 Measurements. North Pacific Marine Science Organization.

Doney, S.C., Fabry, V.J., Feely, R.A., Kleypas, J.A., 2009. Ocean acidification: the other CO2 problem. Annu. Rev. Mar. Sci. 1, 169–192. https://doi.org/10.1146/annurev.marine.010908.163834.

Feely, R.A., 2004. Impact of anthropogenic CO2 on the CaCO3 system in the oceans. Science 305, 362–366. https://doi.org/10.1126/science.1097329.

Frieder, C.A., Applebaum, S.L., Pan, T.C.F., Hedgecock, D., Manahan, D.T., 2016. Metabolic cost of calcification in bivalve larvae under experimental ocean acidification. ICES J. Mar. Sci. 74, 941–954. https://doi.org/10.1093/icesjms/fsw213.

Gac, J.P., Marrec, P., Cariou, T., Guillerm, C., Macé, É., Vernet, M., Bozec, Y., 2020. Cardinal buoys: an opportunity for the study of air-sea CO2 fluxes in coastal ecosystems. Front. Mar. Sci. 7, 712.

Gao, K., Gao, G., Wang, Y., Dupont, S., 2020. Impacts of ocean acidification under multiple stressors on typical organisms and ecological processes. Mar.Life Sci.Technol. 2, 279–291. https://doi.org/10.1007/s42995-020-00048-w.

García, E., Clemente, S., Hernández, J.C., 2015. Ocean warming ameliorates the negative effects of ocean acidification on Paracentrotus lividus larval development and settlement. Mar. Environ. Res. 110, 61–68.

Guo, X., Huang, M., Pu, F., You, W., Ke, C., 2015. Effects of ocean acidification caused by rising CO2 on the early development of three mollusks. Aquat. Biol. 23, 147–157. https://doi.org/10.3354/ab00615.

Guppy, M., Withers, P., 1999. Metabolic depression in animals: physiological perspectives and biochemical generalizations. Biol. Rev. Camb. Philos. Soc. 74, 1–40. https://doi.org/10.1017/s0006323198005258.

Hadfield, M., Paul, V., 2001. Natural chemical cues for settlement and metamorphosis of marine-invertebrate larvae. In: Marine Science. CRC Press, pp. 431–461.

Hamdoun, A., Epel, D., 2007. Embryo stability and vulnerability in an always changing world. Proc. Natl. Acad. Sci. U. S. A. 104, 1745–1750. https://doi.org/10.1073/pnas.0610108104.

Harney, E., Lachambre, S., Roussel, S., Huchette, S., Enez, F., Morvezen, R., Haffray, P., Boudry, P., 2018. Transcriptome based SNP discovery and validation for parentage assignment in hatchery progeny of the European abalone Haliotis tuberculata. Aquaculture 491, 105–113. https://doi.org/10.1016/j.aquaculture.2018.03.006.

Hofmann, L.C., Straub, S., Bischof, K., 2012. Competition between calcifying and noncalcifying temperate marine macroalgae under elevated CO2 levels. Mar. Ecol. Prog. Ser. 464, 89–105. https://doi.org/10.3354/meps09892.

Huchette, S., 2004. Maternal variability in the blacklip abalone, Haliotis rubra leach (Mollusca: Gastropoda): effect of egg size on fertilisation success. Aquaculture 231, 181–195. https://doi.org/10.1016/j.aquaculture.2003.08.027.

Huchette, S., Clavier, J., 2004. Status of the ormer (Haliotis tuberculata L.) industry in Europe. J. Shellfish Res. 23, 951–956.

IPCC, 2014. Summary for policymakers. In: Climate Change 2014: Impacts, Adaptation, and Vulnerability. Part A: Global and Sectoral Aspects. Contribution of Working Group II to the Fifth Assessment Report of the Intergovernmental Panel on Climate Change. Cambridge University Press, Cambridge, United Kingdom and New York, NY, USA 1132 pp.

Jardillier, E., Rousseau, M., Gendron-Badou, A., Fröhlich, F., Smith, D.C., Martin, M., Helléouet, M.N., Huchette, S., Doumenc, D., Auzoux-Bordenave, S., 2008. A morphological and structural study of the larval shell from the abalone Haliotis tuberculata. Mar. Biol. 154, 735–744. https://doi.org/10.1007/s00227-008-0966-3.

Jiang, L., Zhang, F., Guo, M.L., Guo, Y.J., Zhang, Y.Y., Zhou, G.W., Cai, L., Lian, J.S., Qian, P.Y., Huang, H., 2018. Increased temperature mitigates the effects of ocean acidification on the calcification of juvenile Pocillopora damicornis, but at a cost. Coral Reefs 37, 71–79.

Kashiwada, J.V., Taniguchi, I.K., 2007. Application of recent red abalone Haliotis rufescens surveys to management decisions outlined in the California abalone recovery and management plan. J. Shellfish Res. 26, 713–717. https://doi.org/10.2983/0730-8000(2007)26[713:aorrah]2.0.co;2.

Kimura, R.Y.O., Takami, H., Ono, T., Onitsuka, T., Nojiri, Y., 2011. Effects of elevated pCO2 on the early development of the commercially important gastropod, Ezo abalone Haliotis discus hannai. Fish. Oceanogr. 20, 357–366. https://doi.org/10.1111/j.1365-2419.2011.00589.x.

Knights, A.M., Norton, M.J., Lemasson, A.J., Stephen, N., 2020. Ocean acidification mitigates the negative effects of increased sea temperatures on the biomineralization and crystalline ultrastructure of Mytilus. Front. Mar. Sci. 7, 773.

Ko, G.W.K., Dineshram, R., Campanati, C., Chan, V.B.S., Havenhand, J., Thiyagarajan, V., 2014. Interactive effects of ocean acidification, elevated temperature, and reduced salinity on early-life stages of the pacific oyster. Environ. Sci. Technol. 48, 10079–10088. https://doi.org/10.1021/es501611u.

Koch, M., Bowes, G., Ross, C., Zhang, X.-H., 2012. Climate change and ocean acidification effects on seagrasses and marine macroalgae. Glob. Chang. Biol. 19, 103–132. https://doi.org/10.1111/j.1365-2486.2012.02791.x.

Kroeker, K.J., Kordas, R.L., Crim, R., Hendriks, I.E., Ramajo, L., Singh, G.S., Duarte, C.M., Gattuso, J.-P., 2013. Impacts of ocean acidification on marine organisms: quantifying sensitivities and interaction with warming. Glob. Chang. Biol. 19, 1884–1896. https://doi.org/10.1111/gcb.12179.

Kroeker, K.J., Gaylord, B., Hill, T.M., Hosfelt, J.D., Miller, S.H., Sanford, E., 2014. The role of temperature in determining species' vulnerability to ocean acidification: a case study using Mytilus galloprovincialis. PloS one 9, e100353.

Kuffner, I.B., Andersson, A.J., Jokiel, P.L., Rodgers, K.u.S., Mackenzie, F.T., 2008. Decreased abundance of crustose coralline algae due to ocean acidification. Nat. Geosci. 1, 114–117. https://doi.org/10.1038/ngeo100.

Lefevre, S., 2016. Are global warming and ocean acidification conspiring against marine ectotherms? A meta-analysis of the respiratory effects of elevated temperature, high CO2 and their interaction. Conserv Physiol 4, cow009. https://doi.org/10.1093/conphys/cow009.

Leighton, D.L., 1974. The influence of temperature on larval and juvenile growth in three species of southern California abalones. Fish. Bull. 72, 1137–1145.

Li, J., Jiang, Z., Zhang, J., Qiu, J.-W., Du, M., Bian, D., Fang, J., 2013. Detrimental effects of reduced seawater pH on the early development of the Pacific abalone. Mar. Pollut. Bull. 74, 320–324. https://doi.org/10.1016/j.marpolbul.2013.06.035.

Liu, W., He, M., 2012. Effects of ocean acidification on the metabolic rates of three species of bivalve from southern coast of China. Chin. J. Oceanol. Limnol. 30, 206–211. https://doi.org/10.1007/s00343-012-1067-1.

Martin, S., Gattuso, J.-P., 2009. Response of Mediterranean coralline algae to ocean acidification and elevated temperature. Global Change Biol. 15, 2089–2100. https://doi.org/10.1111/j.1365-2486.2009.01874.x.

Mehrbach, C., Culberson, C.H., Hawley, J.E., Pytkowicx, R.M., 1973. Measurement of the apparent dissociation constants of carbonic acid in seawater at atmospheric pressure1.

Limnol. Oceanogr. 18, 897–907. https://doi.org/10.4319/lo.1973.18.6.0897.
Micheli, F., Shelton, A.O., Bushinsky, S.M., Chiu, A.L., Haupt, A.J., Heiman, K.W., Kappel, C.V., Lynch, M.C., Martone, R.G., Dunbar, R.B., Watanabe, J., 2008. Persistence of depleted abalones in marine reserves of central California. Biol. Conserv. 141, 1078–1090. https://doi.org/10.1016/j.biocon.2008.01.014.
Morales-Bojórquez, E., Muciño-Díaz, M.O., Vélez-Barajas, J.A., 2008. Analysis of the decline of the abalone fishery (Haliotis fulgens and H corrugata) along the westcentral coast of the Baja California peninsula,Mexico. 27, 865–870.
Morash, A.J., Alter, K., 2015. Effects of environmental and farm stress on abalone physiology: perspectives for abalone aquaculture in the face of global climate change. Rev. Aquacult. 7, 1–27.
Narita, D., Rehdanz, K., Tol, R.S.J., 2012. Economic costs of ocean acidification: a look into the impacts on global shellfish production. Clim. Chang. 113, 1049–1063. https://doi.org/10.1007/s10584-011-0383-3.
Onitsuka, T., Takami, H., Muraoka, D., Matsumoto, Y., Nakatsubo, A., Kimura, R., Ono, T., Nojiri, Y., 2018. Effects of ocean acidification with pCO2 diurnal fluctuations on survival and larval shell formation of Ezo abalone, Haliotis discus hannai. Mar. Environ. Res. 134, 28–36. https://doi.org/10.1016/j.marenvres.2017.12.015.
Padilla-Gamiño, J.L., Kelly, M.W., Evans, T.G., Hofmann, G.E., 2013. Temperature and CO2 additively regulate physiology, morphology and genomic responses of larval sea urchins, Strongylocentrotus purpuratus. Proc. Biol. Sci. 280, 20130155. https://doi.org/10.1098/rspb.2013.0155.
Parker, L.M., Ross, P.M., O'Connor, W.A., Borysko, L., Raftos, D.A., Pörtner, H.O., 2012. Adult exposure influences offspring response to ocean acidification in oysters. Glob. Change Biol. 18, 82–92.
Parker, L.M., Ross, P.M., O'Connor, W.A., Pörtner, H.O., Scanes, E., Wright, J.M., 2013. Predicting the response of molluscs to the impact of ocean acidification. Biology (Basel) 2, 651–692. https://doi.org/10.3390/biology2020651.
Pawlik, J.R., 1992. Chemical ecology of the settlement of benthic marine invertebrates. Oceanogr. Mar. Biol. Annu. Rev. 30, 273–335.
Pedroso, F.L., 2017. Effects of elevated temperature on the different life stages of tropical mollusk, donkey's ear abalone (Haliotis asinina). Aquacult.Aquar.Conserv.Legis. 10, 1421–1427.
Pörtner, H., 2008. Ecosystem effects of ocean acidification in times of ocean warming: a physiologist's view. Mar. Ecol. Prog. Ser. 373, 203–217. https://doi.org/10.3354/meps07768.
Pörtner, H.O., 2010. Oxygen- and capacity-limitation of thermal tolerance: a matrix for integrating climate-related stressor effects in marine ecosystems. J. Exp. Biol. 213, 881–893. https://doi.org/10.1242/jeb.037523.
Przeslawski, R., Byrne, M., Mellin, C., 2015. A review and meta-analysis of the effects of multiple abiotic stressors on marine embryos and larvae. Glob. Change Biol. 21, 2122–2140.
Qui-Minet, Z.N., Delaunay, C., Grall, J., Six, C., Cariou, T., Bohner, O., Legrand, E., Davoult, D., Martin, S., 2018. The role of local environmental changes on maerl and its associated non-calcareous epiphytic flora in the Bay of Brest. Estuar. Coast. Shelf Sci. 208, 140–152.
Rivest, E.B., Hofmann, G.E., 2014. Responses of the metabolism of the larvae of Pocillopora damicornis to ocean acidification and warming. PLoS One 9, e96172. https://doi.org/10.1371/journal.pone.0096172.
Roberts, R.D., Nicholson, C.M., 1997. Variable response from abalone larvae (Haliotis iris, H. virginea) to a range of settlement cues. Molluscan Res. 18, 131–141. https://doi.org/10.1080/13235818.1997.10673687.
Roberts, R.D., Kaspar, H.F., Barker, R.J., 2004. Settlement of abalone (Haliotis iris) larvae in response to five species of coralline algae. J. Shellfish Res. 23, 975–988.
Rodolfo-Metalpa, R., Houlbrèque, F., Tambutté, É., Boisson, F., Baggini, C., Patti, F.P., Jeffree, R., Fine, M., Foggo, A., Gattuso, J.P., Hall-Spencer, J.M., 2011. Coral and mollusc resistance to ocean acidification adversely affected by warming. Nat. Clim. Chang. 1, 308–312.
Rodriguez, S.R., Ojeda, F.P., Inestrosa, N.C., 1993. Settlement of benthic marine invertebrates. Mar. Ecol. Prog. Ser. 97, 193–207. https://doi.org/10.3354/meps097193.
Rosenberg, G., 2014. A new critical estimate of named species-level diversity of the recent mollusca. Am. Malacol. Bull. 32, 308. https://doi.org/10.4003/006.032.0204.
Santander, S.M.S., 2018. CO2-induced pH reduction hinders shell development of early larvae donkey's ear abalone Haliotis asinina (linnaeus 1758). Asian Fish. Sci. 31. https://doi.org/10.33997/j.afs.2018.31.2.002.
Searcy-Bernal, R., Salas-Garza, A.E., Flores-Aguilar, R.A., Hinojosa-Rivera, P.R., 1992. Simultaneous comparison of methods for settlement and metamorphosis induction in the red abalone (Haliotis rufescens). Aquaculture 105, 241–250. https://doi.org/10.1016/0044-8486(92)90090-8.
Slattery, M., 1992. Larval settlement and juvenile survival in the red abalone (Haliotis rufescens), an examination of inductive cues and substrate selection. Aquaculture 102, 143–153. https://doi.org/10.1016/0044-8486(92)90296-w.
Swezey, D.S., Boles, S.E., Aquilino, K.M., Stott, H.K., Bush, D., Whitehead, A., Rogers-Bennett, L., Hill, T.M., Sanford, E., 2020. Evolved differences in energy metabolism and growth dictate the impacts of ocean acidification on abalone aquaculture. PNAS 117, 26513–26519.
Tahil, A.S., Dy, D.T., 2016. Effects of reduced pH on the early larval development of hatchery-reared Donkey's ear abalone, Haliotis asinina (Linnaeus 1758). Aquaculture 459, 137–142. https://doi.org/10.1016/j.aquaculture.2016.03.027.
Talmage, S.C., Gobler, C.J., 2011. Effects of elevated temperature and carbon dioxide on the growth and survival of larvae and juveniles of three species of northwest Atlantic bivalves. PLoS One 6, e26941. https://doi.org/10.1371/journal.pone.0026941.
Thiyagarajan, V., Ko, G.W.K., 2012. Larval growth response of the Portuguese oyster (Crassostrea angulata) to multiple climate change stressors. Aquaculture 370–371, 90–95. https://doi.org/10.1016/j.aquaculture.2012.09.025.
Travers, M.-A., Basuyaux, O., Le GoÏC, N., Huchette, S., Nicolas, J.-L., Koken, M., Paillard, C., 2009. Influence of temperature and spawning effort on Haliotis tuberculata mortalities caused by Vibrio harveyi: an example of emerging vibriosis linked to global warming. Glob. Chang. Biol. 15, 1365–1376. https://doi.org/10.1111/j.1365-2486.2008.01764.x.
Waldbusser, G.G., Hales, B., Langdon, C.J., Haley, B.A., Schrader, P., Brunner, E.L., Gray, M.W., Miller, C.A., Gimenez, I., Hutchinson, G., 2015. Ocean acidification has multiple modes of action on bivalve larvae. PLoS One 10, e0128376. https://doi.org/10.1371/journal.pone.0128376.
Wessel, N., Martin, S., Badou, A., Dubois, P., Huchette, S., Julia, V., Nunes, F., Harney, E., Paillard, C., Auzoux-Bordenave, S., 2018. Effect of CO2–induced ocean acidification on the early development and shell mineralization of the European abalone (Haliotis tuberculata). J. Exp. Mar. Biol. Ecol. 508, 52–63. https://doi.org/10.1016/j.jembe.2018.08.005.
Williams, E.A., Craigie, A., Yeates, A., Degnan, S.M., 2008. Articulated coralline algae of the genus amphiroa are highly effective natural inducers of settlement in the tropical abalone Haliotis asinina. Biol. Bull. 215, 98–107. https://doi.org/10.2307/25470687.
Zippay, M.L., Hofmann, G.E., 2010. Effect of pH on gene expression and thermal tolerance of early life history stages of red abalone (Haliotis rufescens). J. Shellfish Res. 29, 429–439. https://doi.org/10.2983/035.029.0220.
Zittier, Z.M.C., Bock, C., Sukhotin, A.A., Häfker, N.S., Pörtner, H.O., 2018. Impact of ocean acidification on thermal tolerance and acid–base regulation of Mytilus edulis from the White Sea. Polar Biol. 41, 2261–2273.